



JOHANNES GUTENBERG
UNIVERSITÄT MAINZ



3D NUCLEON TOMOGRAPHY WORKSHOP

Modeling and Extraction Methodology

March 15-17 • Jefferson Lab
Newport News, Virginia

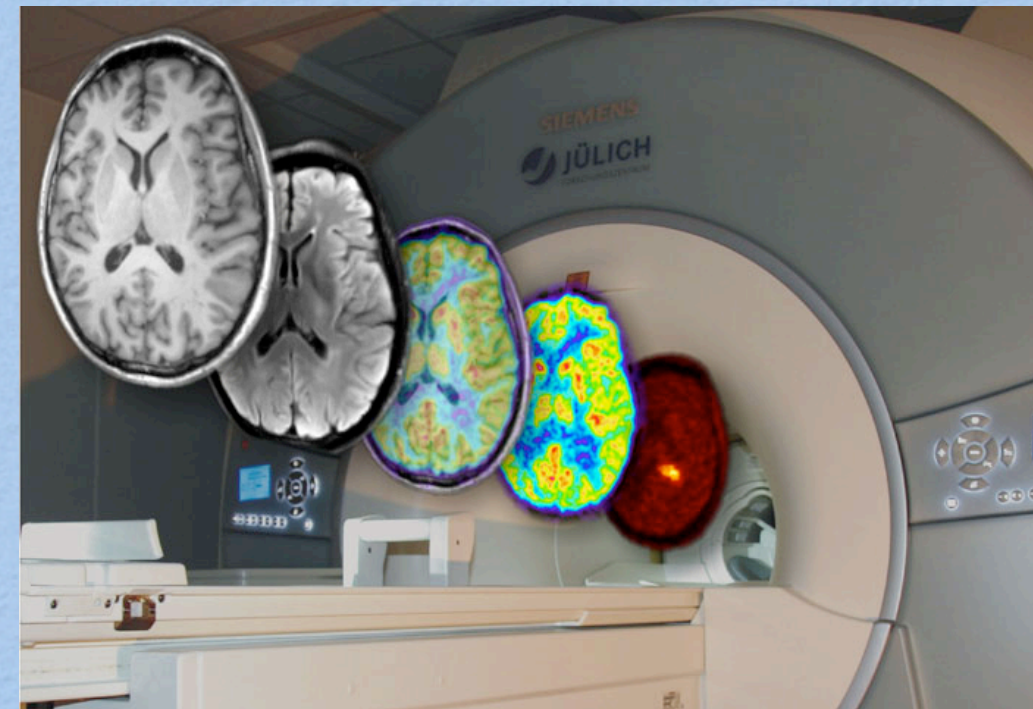
Organizing Committee

- Amber Boehnlein (Jefferson Lab)
- Latifa Elouadrhiri (Jefferson Lab)
- David Richards (Jefferson Lab)
- Franck Sabatié (CEA/Saclay)
- Peter Schweitzer (U. of Connecticut)

Jefferson Lab

www.jlab.org/conferences/3Dmodeling

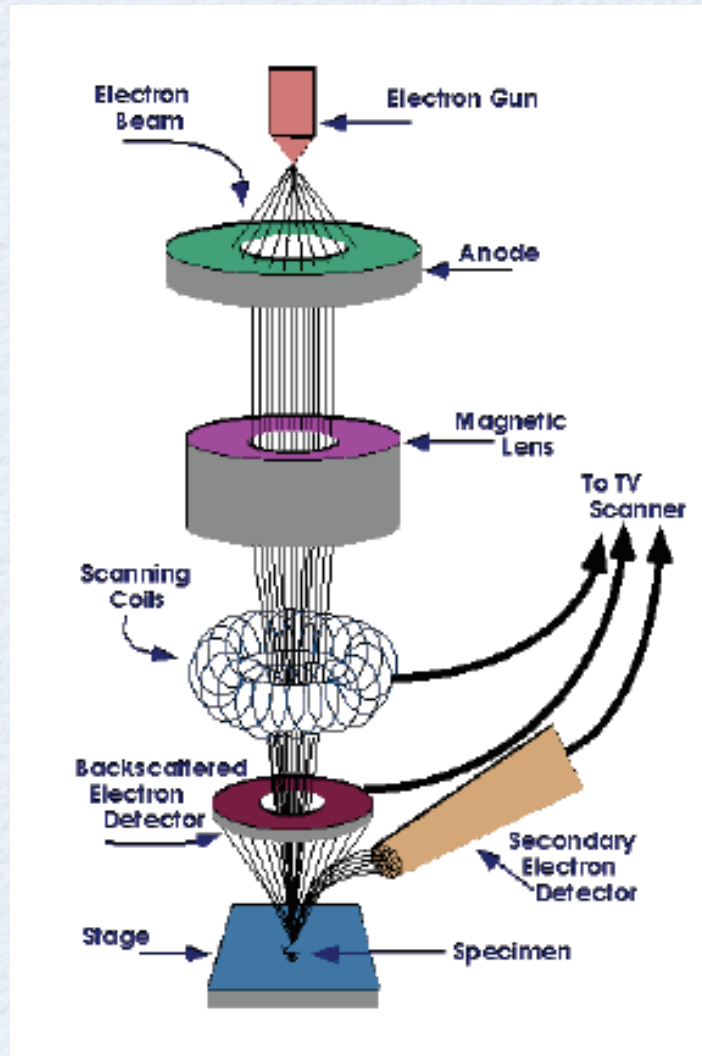
GPDs
and
DVCS



Marc Vanderhaeghen

Jefferson Lab, March 15-17, 2017

how to image a system



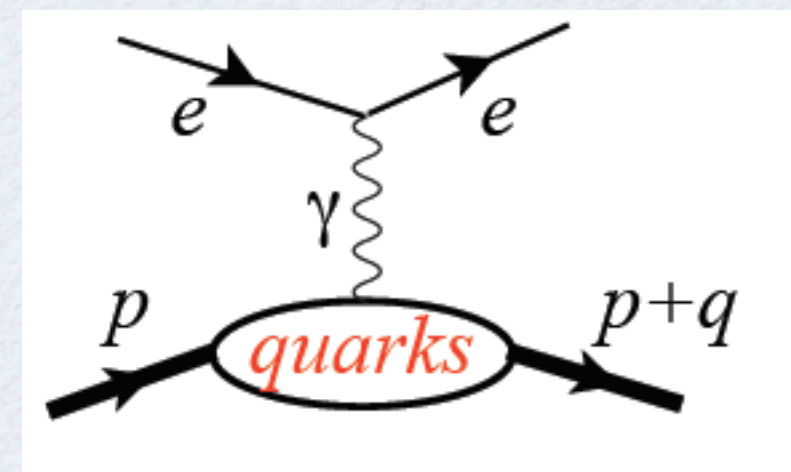
electron microscopy



when target is static ($m_{\text{constituent}}, m_{\text{target}} \gg Q$)

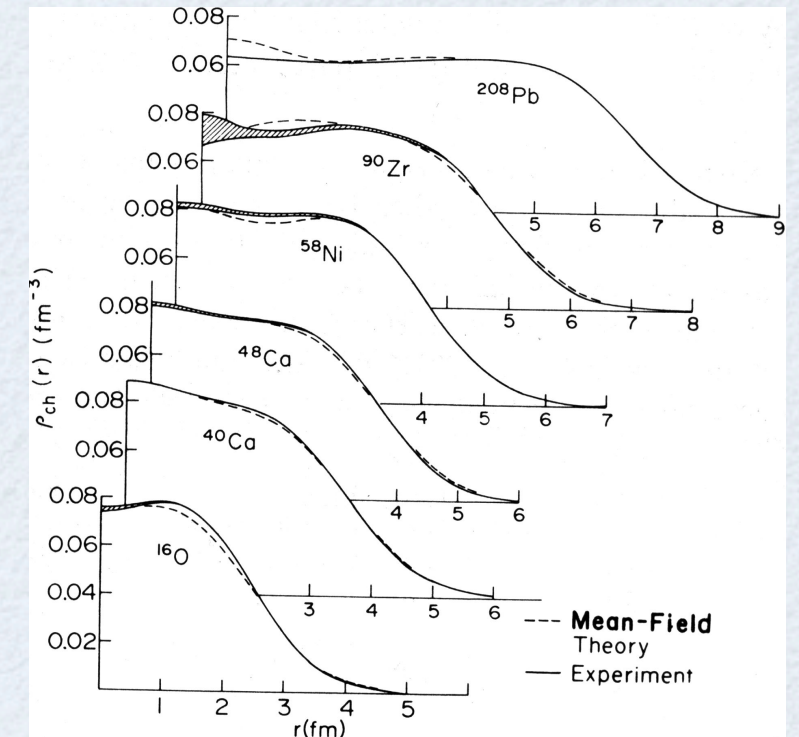
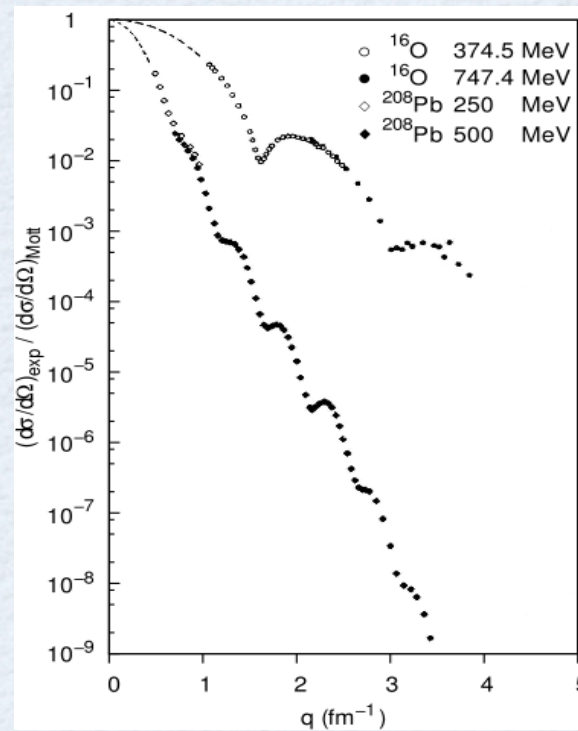
the 3-dim **Fourier transform** of **form factors** gives

the distribution of electric charge and magnetization

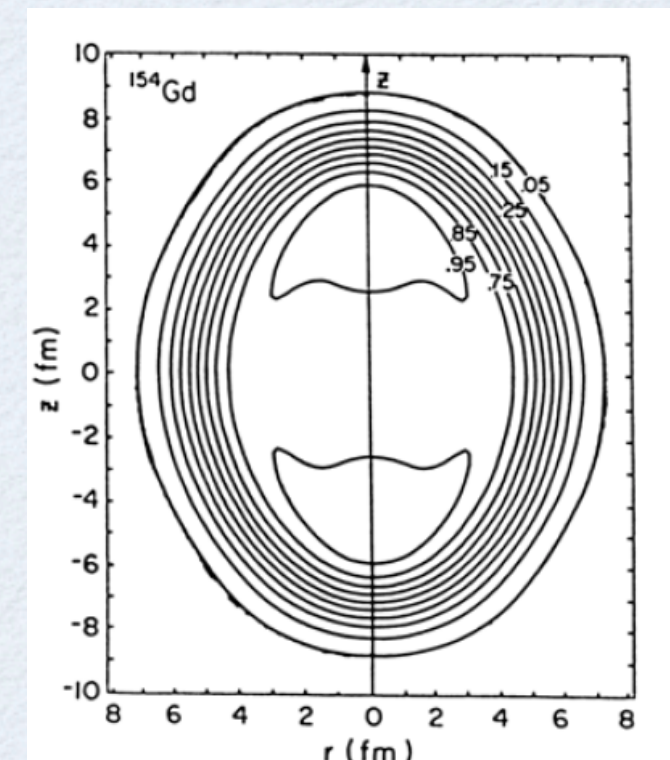
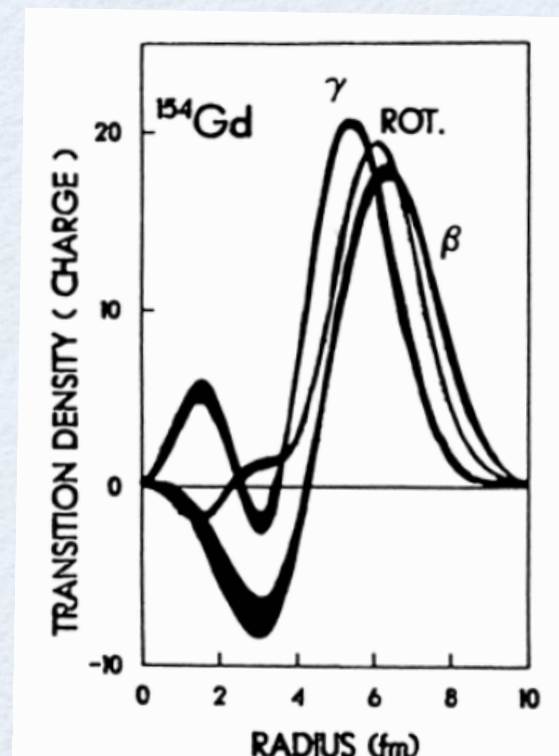


what do we know about spatial distributions of charges in nuclei?

sizes of nuclei:
as revealed through
elastic electron scattering

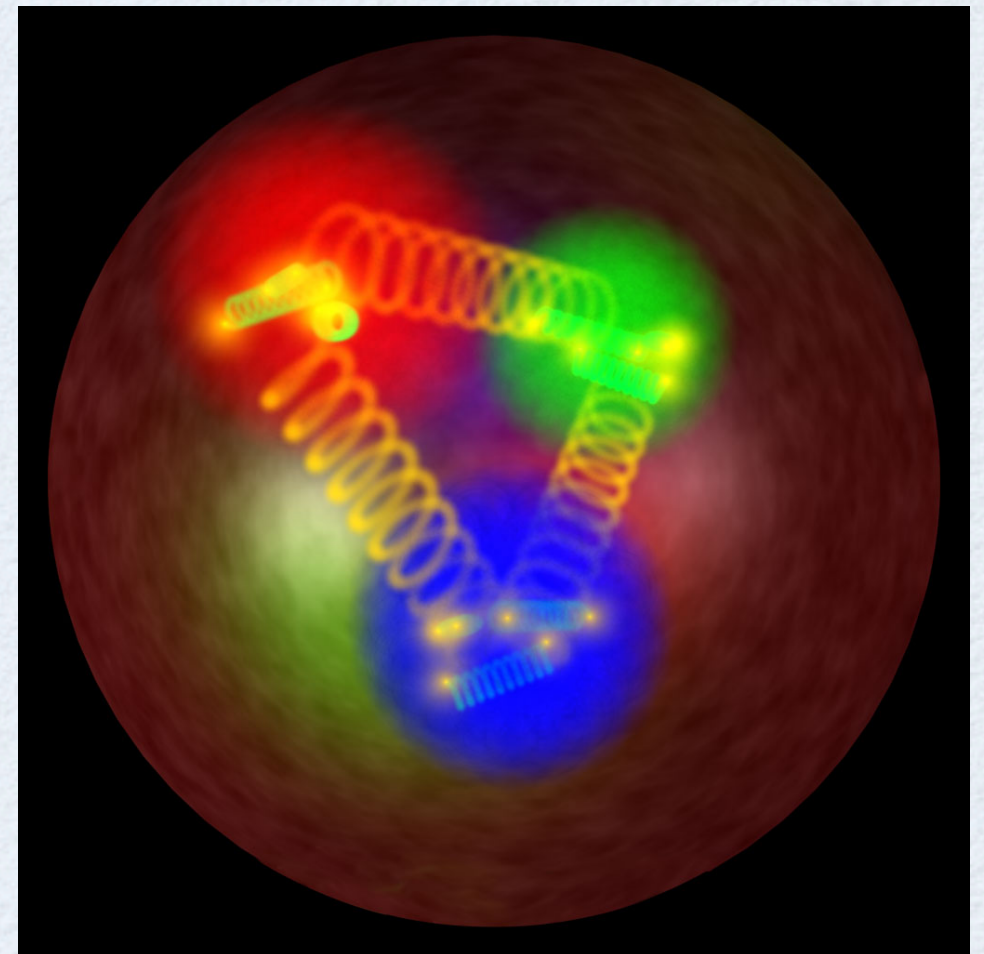


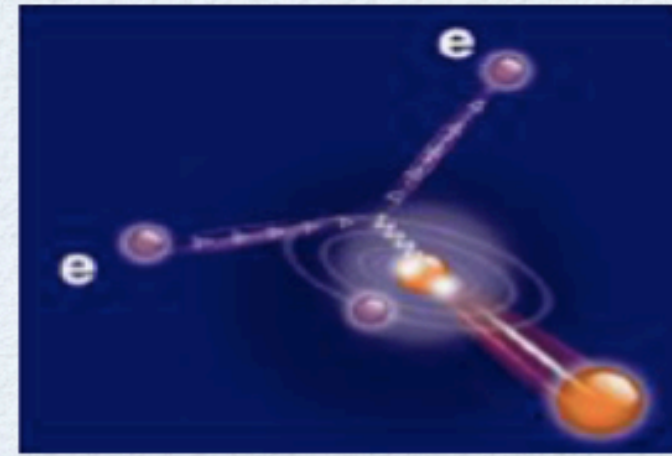
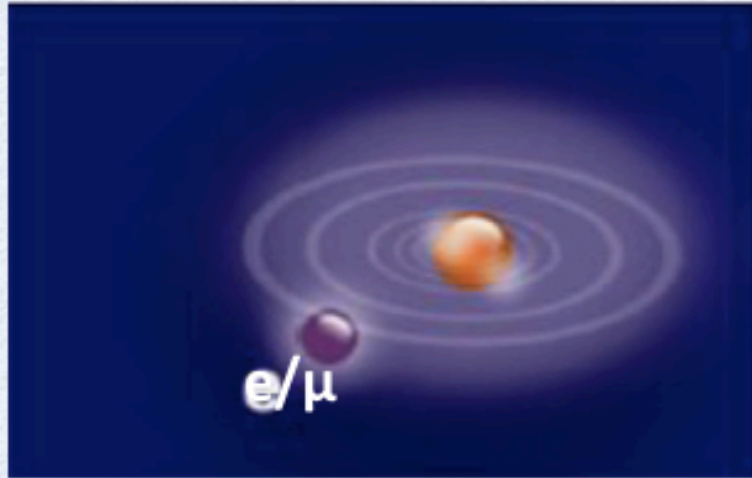
shapes of nuclei:
as revealed through
inelastic electron scattering



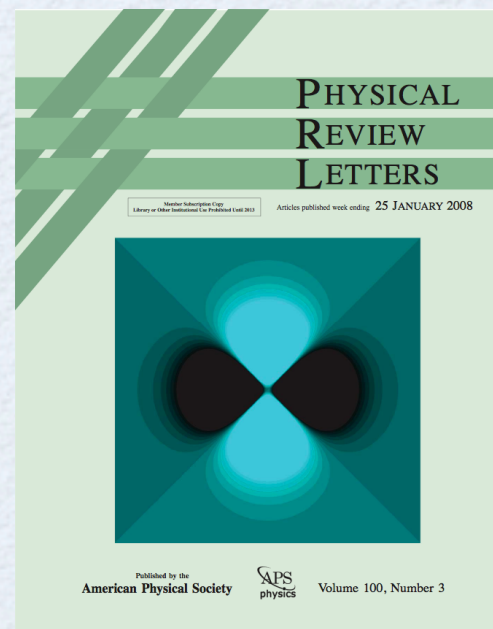
what do we know about the proton size and its charge distributions?

- ➔ proton **size**: charge radius R_E
very low Q^2 **elastic** electron scattering,
atomic spectroscopy (Lamb shift)
- ➔ proton **spatial (charge) distributions**
elastic electron scattering
e.m. FFs: $F_1(Q^2) \rightarrow \rho(\mathbf{b})$
- ➔ proton **3D transverse spatial/
longitudinal momentum distributions**
deeply virtual Compton scattering
GPDs $H(x, \xi, t) \rightarrow \rho(x, \mathbf{b})$ for $\xi=0$

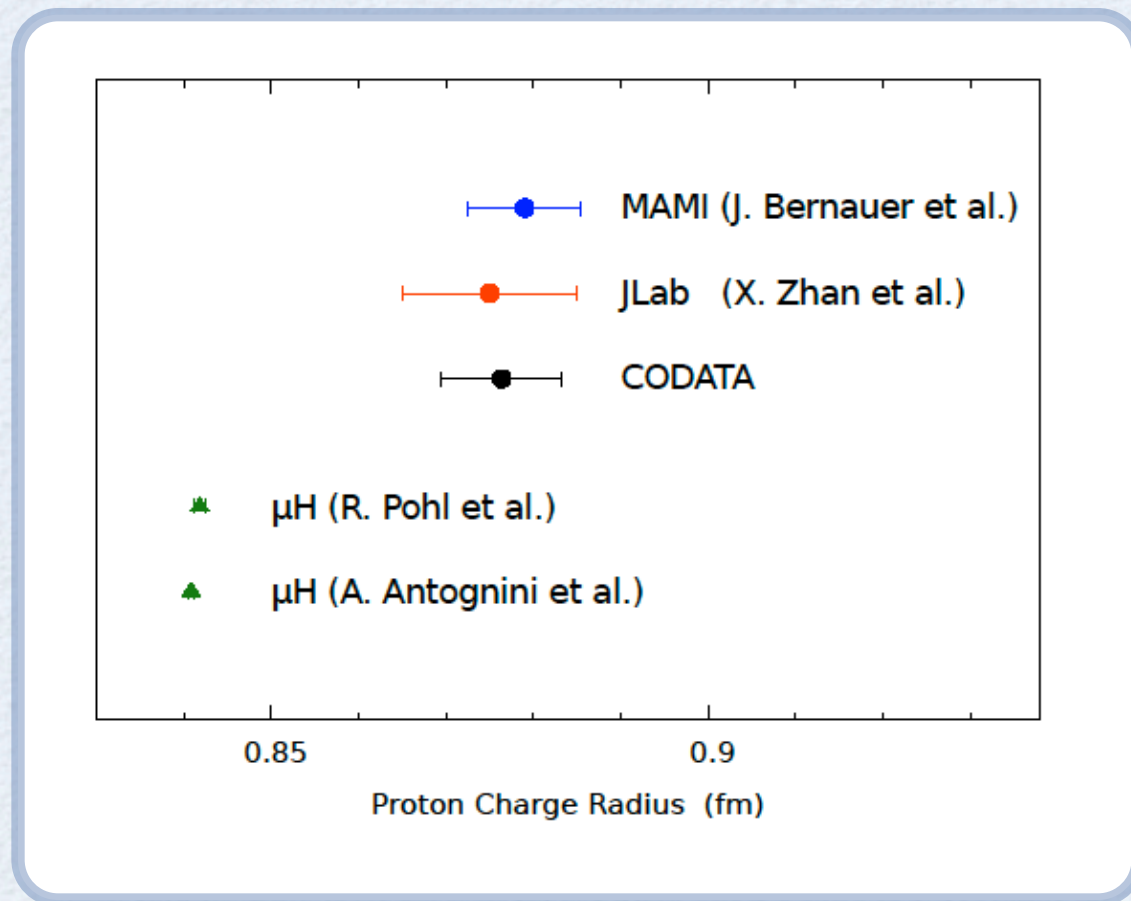




proton size,
proton e.m. form factors,
charge distributions



Proton radius puzzle



μH data:

$$R_E = 0.8409 \pm 0.0004 \text{ fm}$$

Pohl et al. (2010)

Antognini et al. (2013)



7σ difference !?

ep data:

$$R_E = 0.8775 \pm 0.0051 \text{ fm}$$

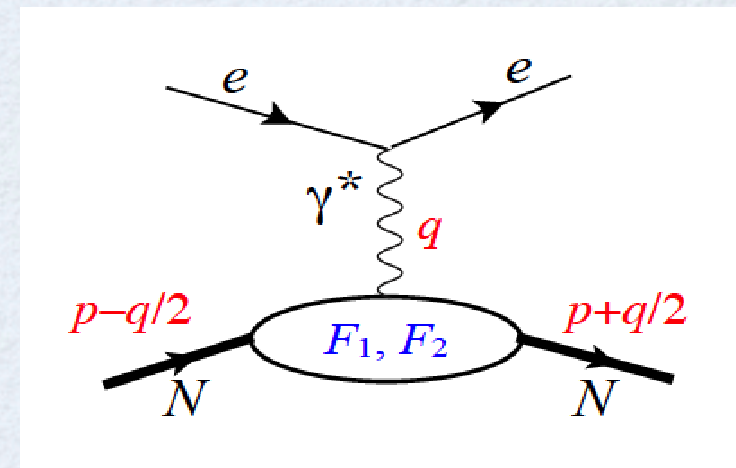
CODATA (2012)



spin-1/2 electromagnetic form factors

➔ **(in)elastic electron scattering** is our microscope to investigate hadron structure

➔ in the **1-photon exchange approximation**:



nucleon (spin 1/2 target) structure is parameterized by 2 **form factors (FFs)**

$$\langle p + \frac{q}{2}, \lambda' | J^\mu(0) | p - \frac{q}{2}, \lambda \rangle = \bar{u}(p + \frac{q}{2}, \lambda') \left[F_1(Q^2) \gamma^\mu + F_2(Q^2) \frac{i}{2M} \sigma^{\mu\nu} q_\nu \right] u(p - \frac{q}{2}, \lambda)$$

↑
Dirac FF

↑
Pauli FF

for proton: $F_1(Q^2 = 0) = 1$ $F_2(Q^2 = 0) = \kappa_p = 1.79$

➔ equivalently: in experiment one often uses **Sachs FFs** with $\tau \equiv \frac{Q^2}{4M^2}$

$$\begin{aligned} G_M(Q^2) &= F_1(Q^2) + F_2(Q^2) && \longrightarrow \text{magnetic FF} \\ G_E(Q^2) &= F_1(Q^2) - \tau F_2(Q^2) && \longrightarrow \text{electric FF} \end{aligned}$$

$$G_E(Q^2) = 1 - \frac{1}{6} \langle r_E^2 \rangle Q^2 + \mathcal{O}(Q^4)$$

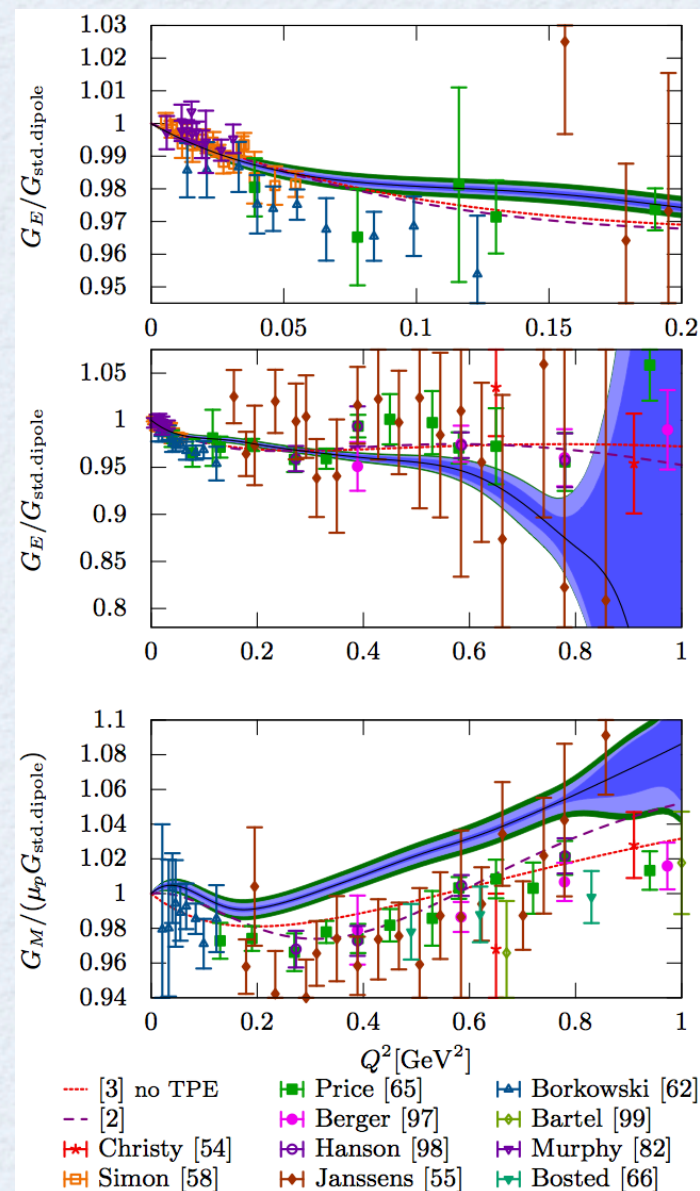
↑
charge radius

e^- scattering cross sections

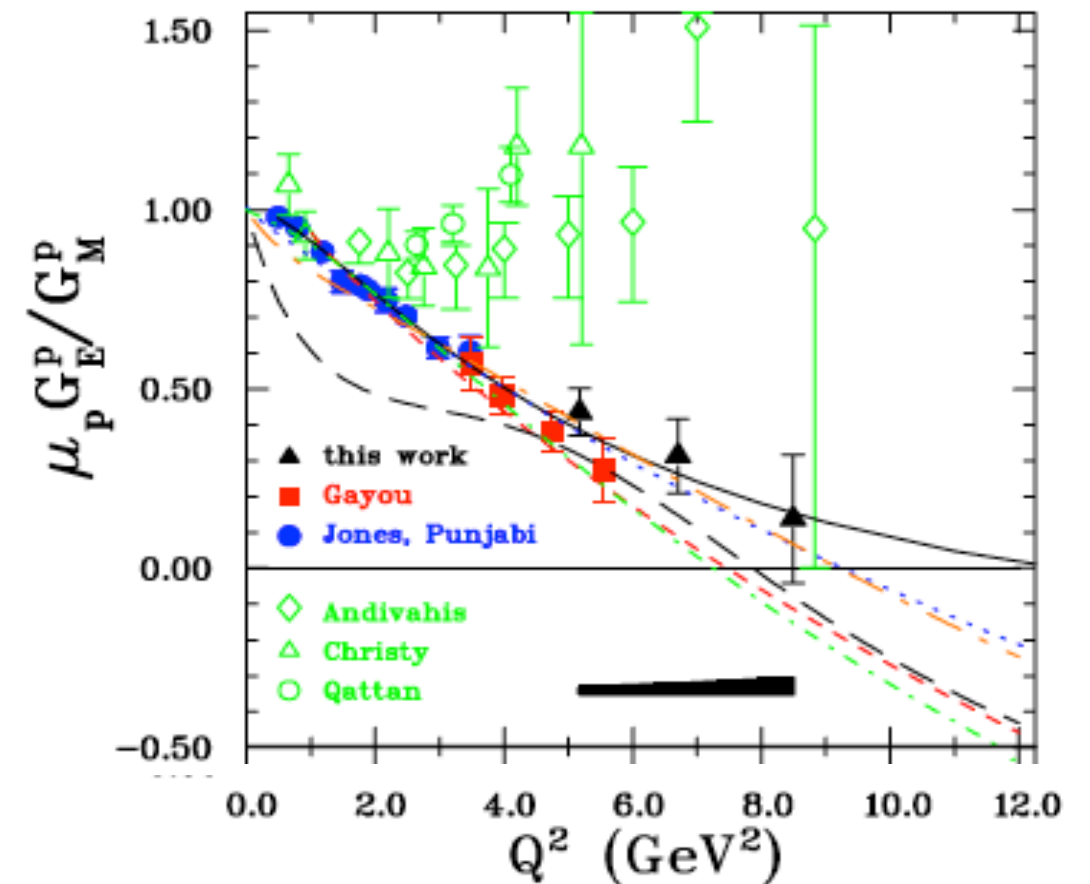
Electron scattering facilities JLab (12 GeV), MAMI (1.6 GeV):
uniquely positioned to deliver high precision data

MAMI/A1 achieved $< 1\%$ measurement
of proton charge radius R_E

JLab polarization transfer measurements:
 G_{Ep} / G_{Mp} difference with Rosenbluth



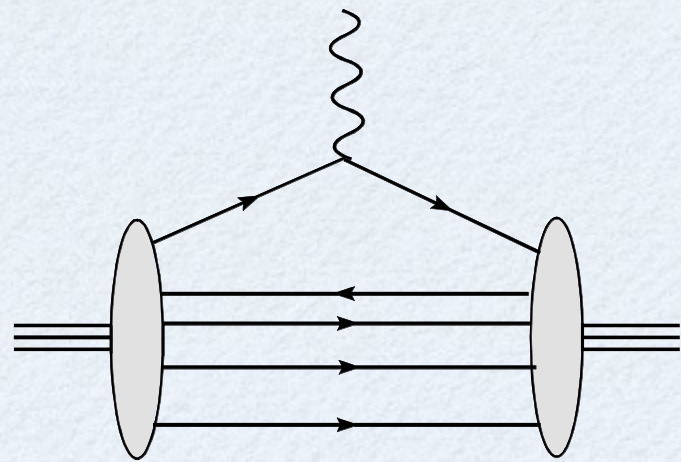
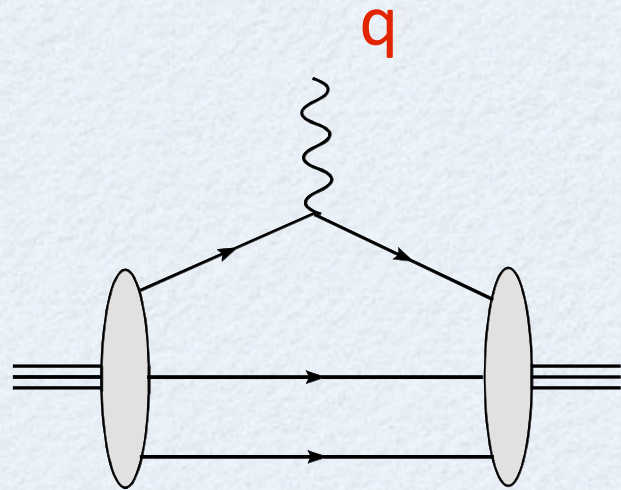
Bernauer et al. (2010, 2013)



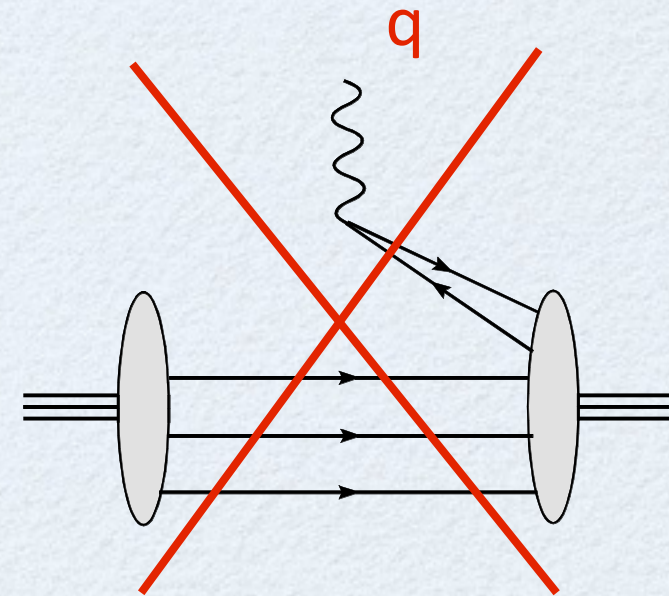
Jones et al. (2000) Punjabi et al. (2005)

Gayou et al. (2002) Puckett et al. (2010)

Interpretation of form factor as quark density



overlap of wave function
Fock components
with **same** number of quarks



overlap of wave function
Fock components
with **different** number of quarks
NO probability / charge density
interpretation

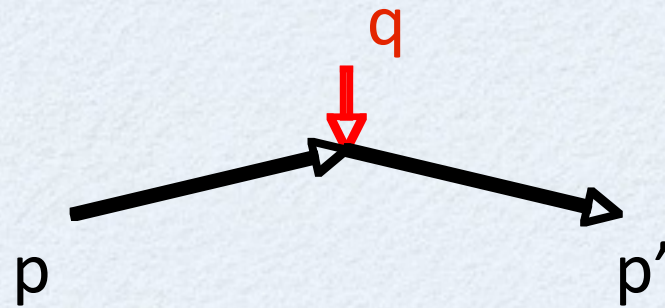
absent in a light-front frame!

$$q^+ = q^0 + q^3 = 0$$

quark transverse charge densities in nucleon (1)

→ light-front

$$q^+ = q^0 + q^3 = 0$$

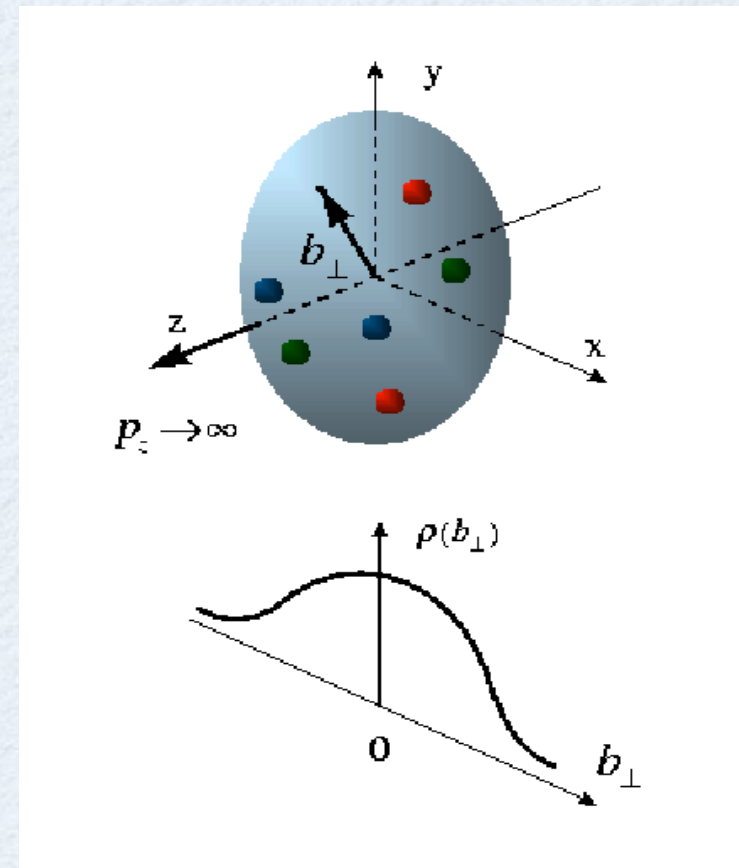


photon only couples to forward moving quarks

→ quark charge density operator

$$J^+ = J^0 + J^3 = \bar{q}\gamma^+q = 2q_+^\dagger q_+$$

with $q_+ \equiv \frac{1}{4}\gamma^-\gamma^+q$



→ longitudinally polarized nucleon

$$\begin{aligned} \rho_0^N(\vec{b}) &\equiv \int \frac{d^2\vec{q}_\perp}{(2\pi)^2} e^{-i\vec{q}_\perp \cdot \vec{b}} \frac{1}{2P^+} \langle P^+, \frac{\vec{q}_\perp}{2}, \lambda | J^+(0) | P^+, -\frac{\vec{q}_\perp}{2}, \lambda \rangle \\ &= \int_0^\infty \frac{dQ}{2\pi} Q J_0(bQ) F_1(Q^2) \end{aligned}$$

Soper (1997)

Burkardt (2000)

Miller (2007)

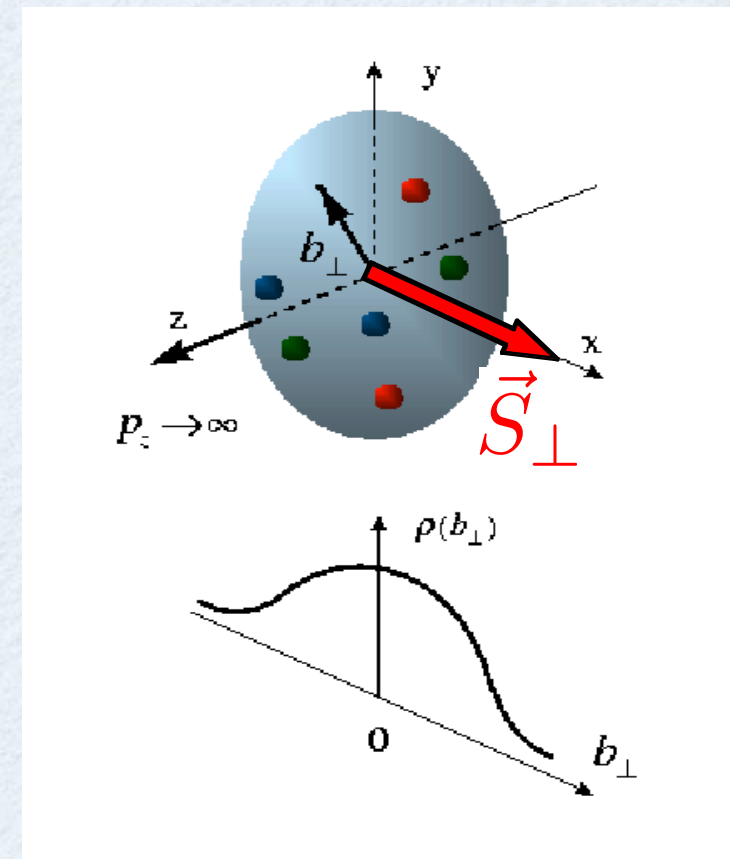
quark transverse charge densities in nucleon (2)

→ transversely polarized nucleon

transverse spin $\vec{S}_\perp = \cos \phi_S \hat{e}_x + \sin \phi_S \hat{e}_y$

e.g. along x-axis $\phi_S = 0$

$$\vec{b} = b(\cos \phi_b \hat{e}_x + \sin \phi_b \hat{e}_y)$$



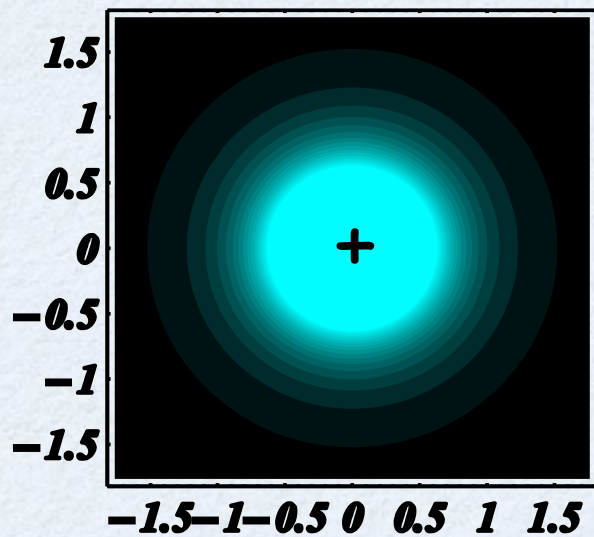
$$\begin{aligned} \rho_T^N(\vec{b}) &\equiv \int \frac{d^2 \vec{q}_\perp}{(2\pi)^2} e^{-i\vec{q}_\perp \cdot \vec{b}} \frac{1}{2P^+} \langle P^+, \frac{\vec{q}_\perp}{2}, s_\perp = +\frac{1}{2} | J^+(0) | P^+, -\frac{\vec{q}_\perp}{2}, s_\perp = +\frac{1}{2} \rangle \\ &= \rho_0^N(b) + \sin(\phi_b - \phi_S) \int_0^\infty \frac{dQ}{2\pi} \frac{Q^2}{2M} J_1(bQ) F_2(Q^2) \end{aligned}$$

↑ dipole field pattern

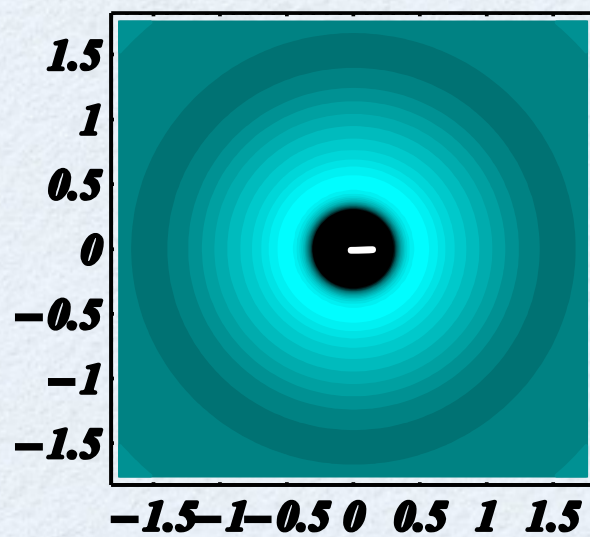
Carlson, Vdh (2007)

spatial imaging of hadrons

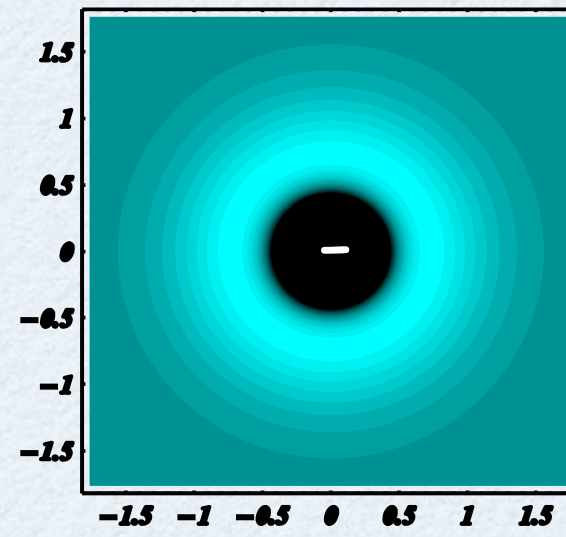
proton



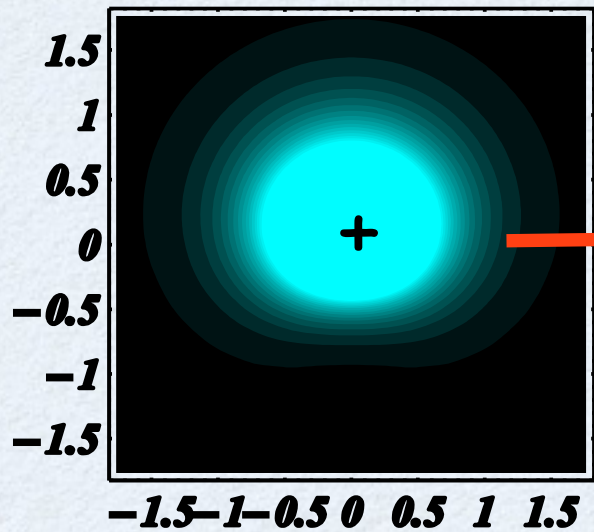
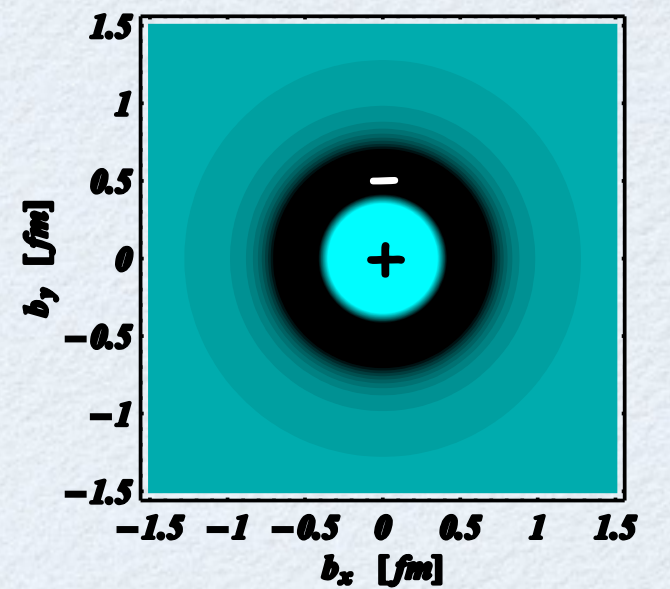
neutron



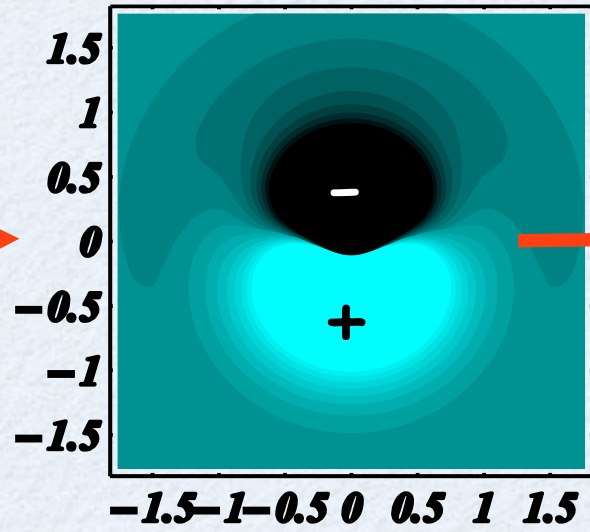
$p \rightarrow \Delta^+$



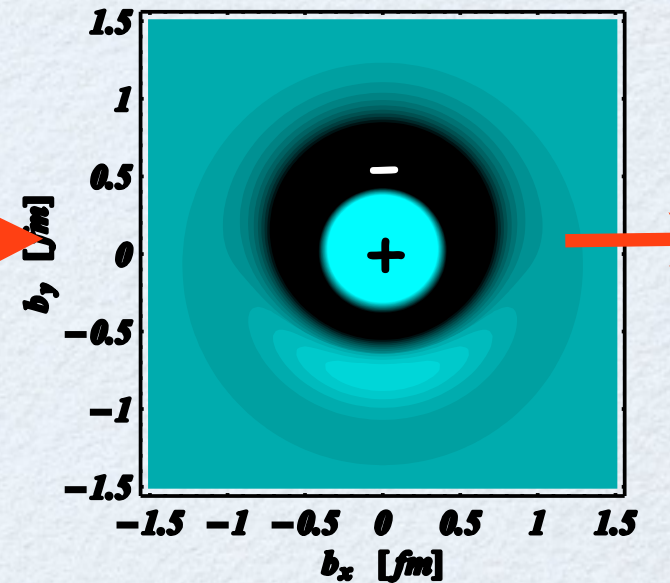
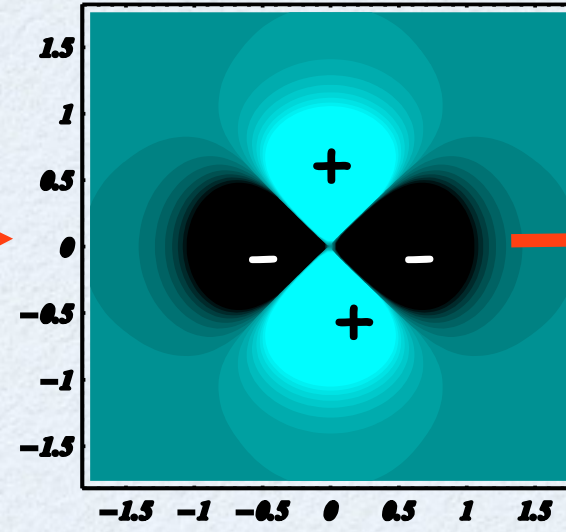
$p \rightarrow N^* (1440)$



Miller (2007)

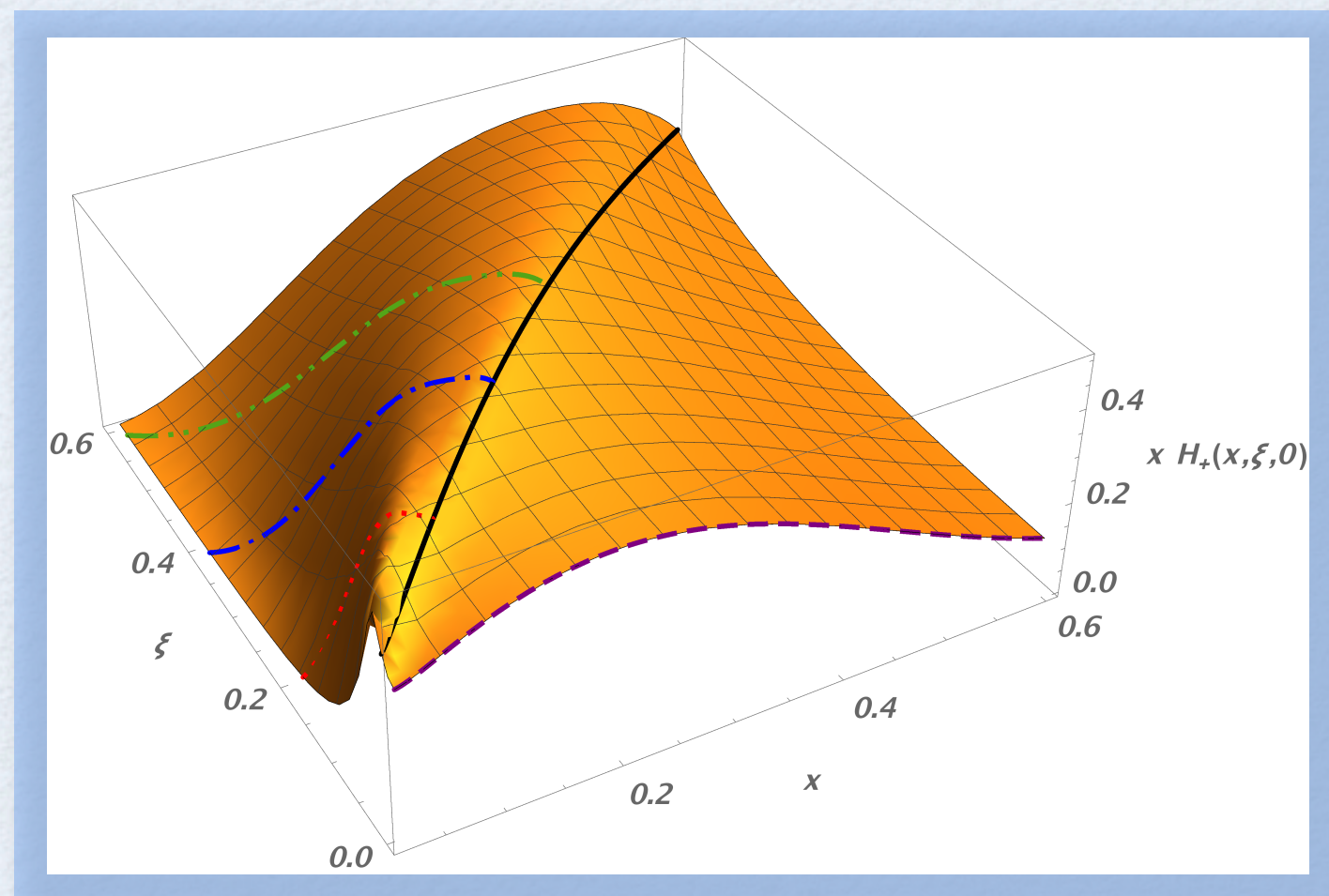


Carlson, Vdh (2007)



Tiator, Vdh (2007)

Generalized Parton Distributions and DVCS



Correlations in transverse position/longitudinal momentum

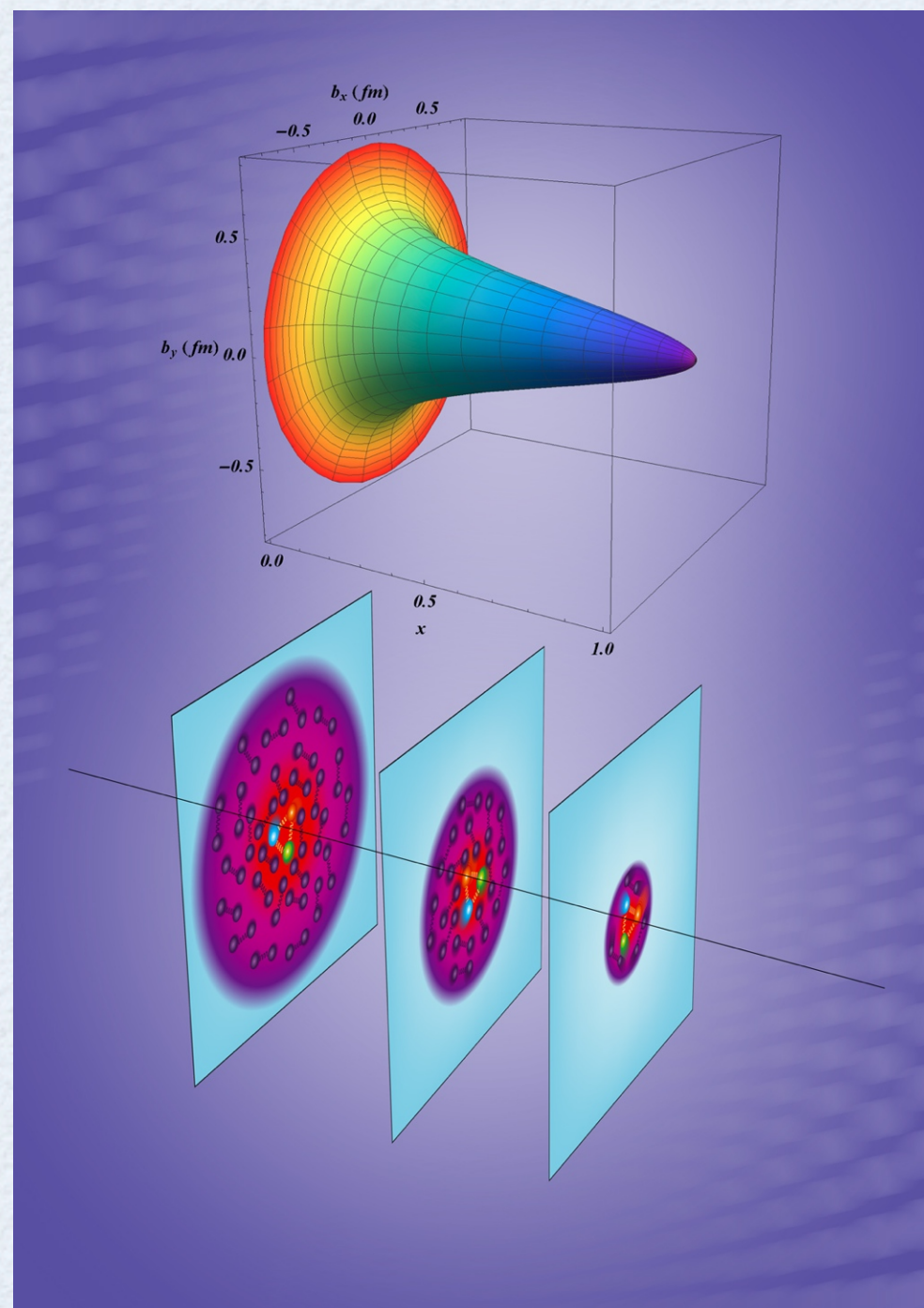
**elastic
scattering**



DIS

quark
distributions in
transverse
position space

quark
distributions in
longitudinal
momentum



proton
3D imaging

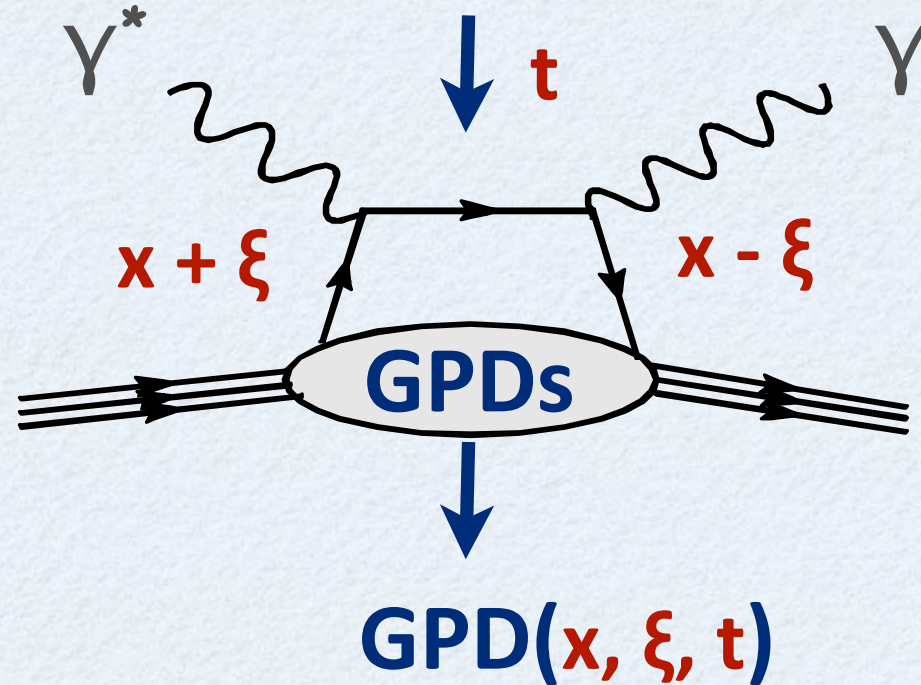
Burkardt (2000, 2003)

Belitsky, Ji, Yuan
(2004)

DVCS: tool to access GPDs

world data on proton F_2

$Q^2 \gg 1 \text{ GeV}^2$



➔ at large Q^2 : QCD factorization theorem

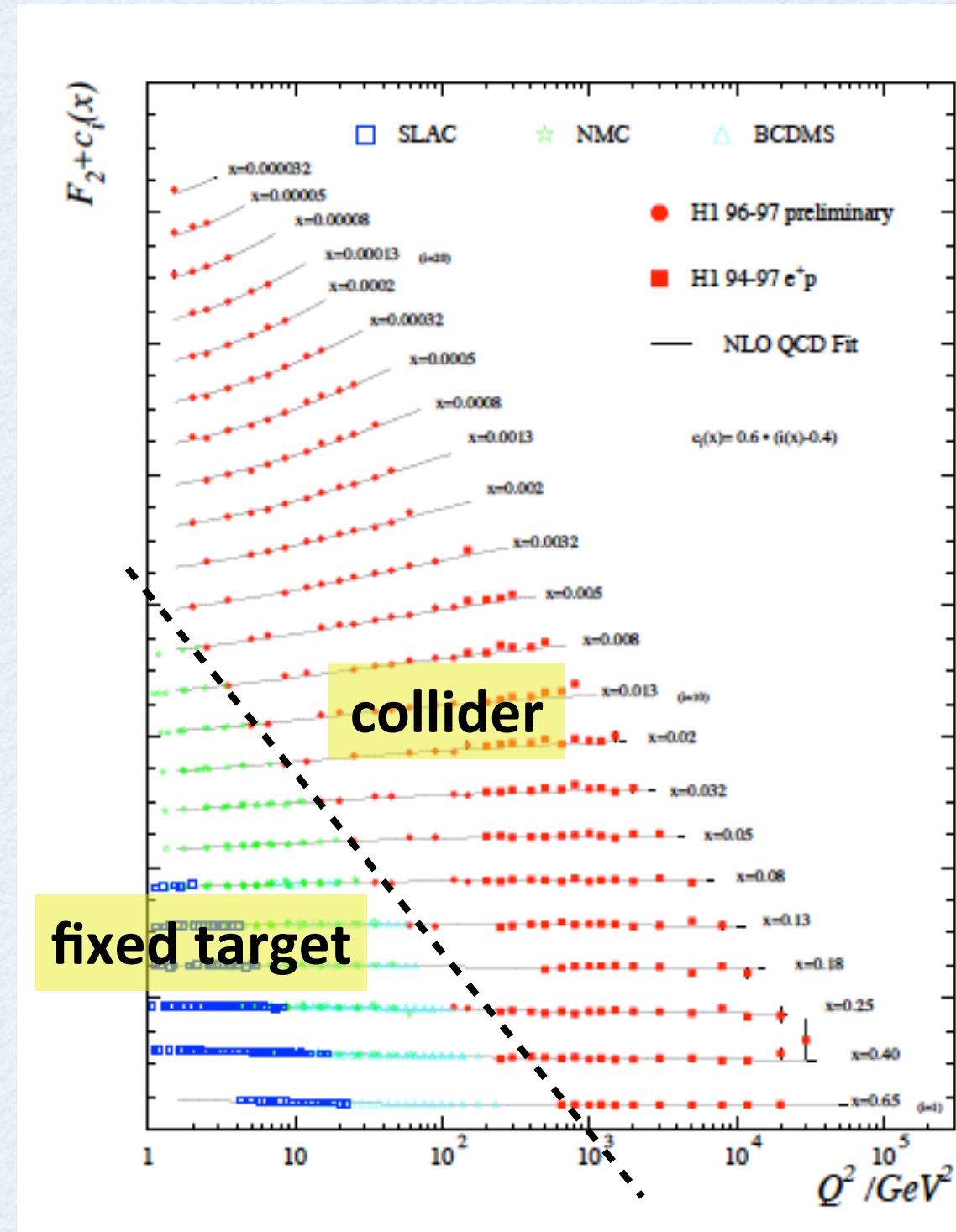
Müller et al (1994)

Ji (1995) Radyushkin (1995)

Collins, Frankfurt, Strikman (1996)

at twist-2: 4 quark helicity conserving GPDs

➔ key: Q^2 leverage needed to test QCD scaling



GPDs: known limits

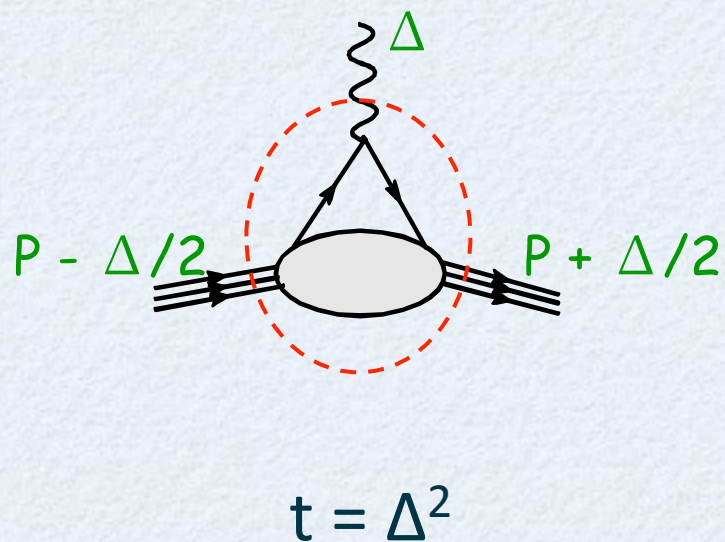
→ in forward kinematics ($\xi=0, t=0$) : **PDF limit**

$$H^q(x, \xi = 0, t = 0) = q(x)$$

$$\tilde{H}^q(x, \xi = 0, t = 0) = \Delta q(x)$$

E, \tilde{E}^q do not appear in forward kinematics (DIS) → **new information**

→ first moments of GPDs : **elastic form factor limit**



$$\int_{-1}^{+1} dx H^q(x, \xi, t) = F_1^q(t)$$

→ Dirac FF

$$\int_{-1}^{+1} dx E^q(x, \xi, t) = F_2^q(t)$$

→ Pauli FF

$$\int_{-1}^{+1} dx \tilde{H}^q(x, \xi, t) = G_A^q(t)$$

→ axial FF

$$\int_{-1}^{+1} dx \tilde{E}^q(x, \xi, t) = G_P^q(t)$$

→ pseudoscalar FF

GPDs: higher moments, total quark angular momentum



$$\int_{-1}^{+1} dx x H^q(x, \xi, t) = A(t)(t) + \xi^2 C(t)(t)$$

$$\int_{-1}^{+1} dx x E^q(x, \xi, t) = B(t)(t) - \xi^2 C(t)(t)$$

form factors of energy-momentum tensor

Polyakov, Weiss (1999)

Polyakov (2003)

Goeke, Schweitzer et al. (2007)



Ji's angular momentum sum rule

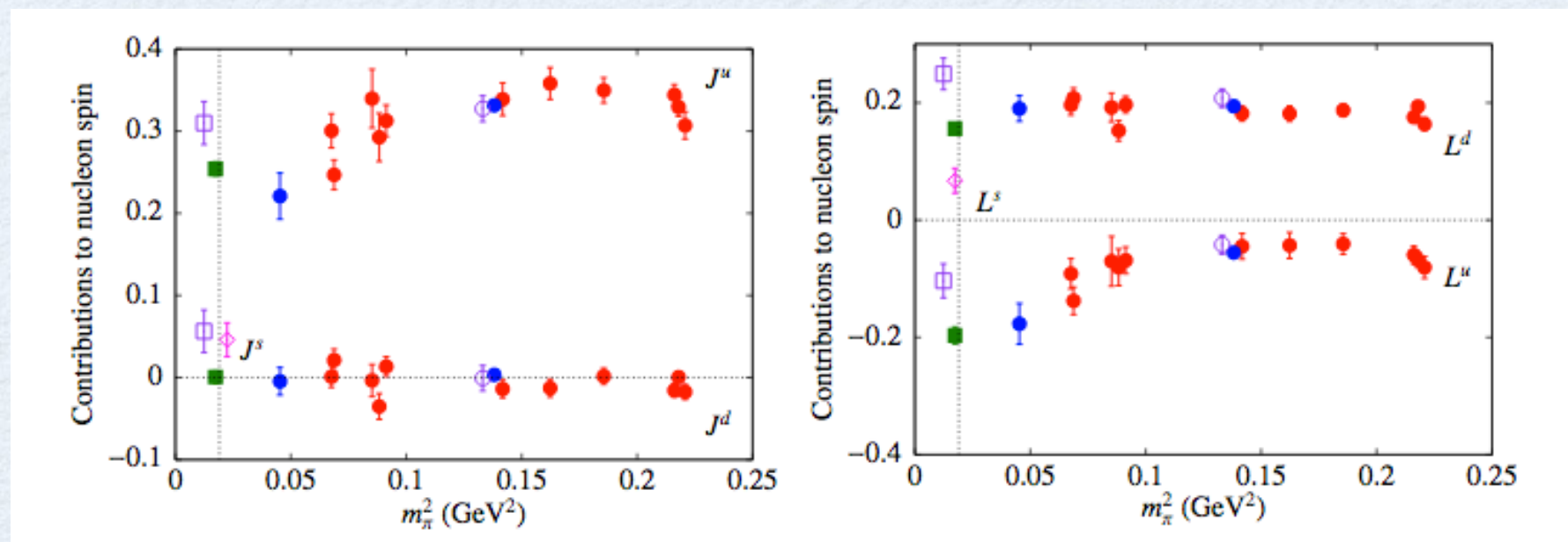
$$\int_{-1}^{+1} dx x \{ H^q(x, \xi, 0) + E^q(x, \xi, 0) \} = A(0) + B(0) = 2J^q$$



lattice QCD calculations at the physical point

e.g. twisted mass fermions

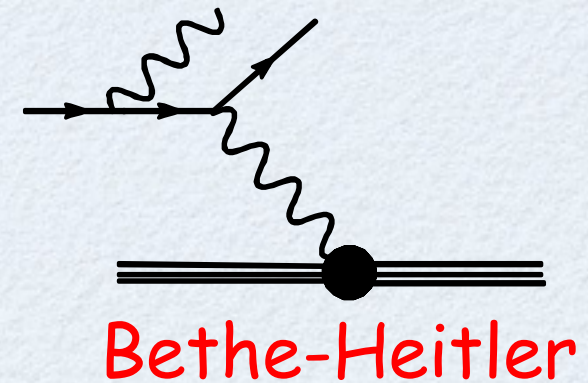
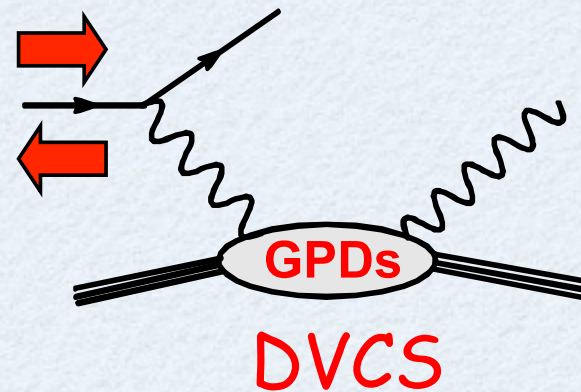
Alexandrou et al. (2016)



d, s-quarks carry very small total angular momentum, u-quark carries around 50%

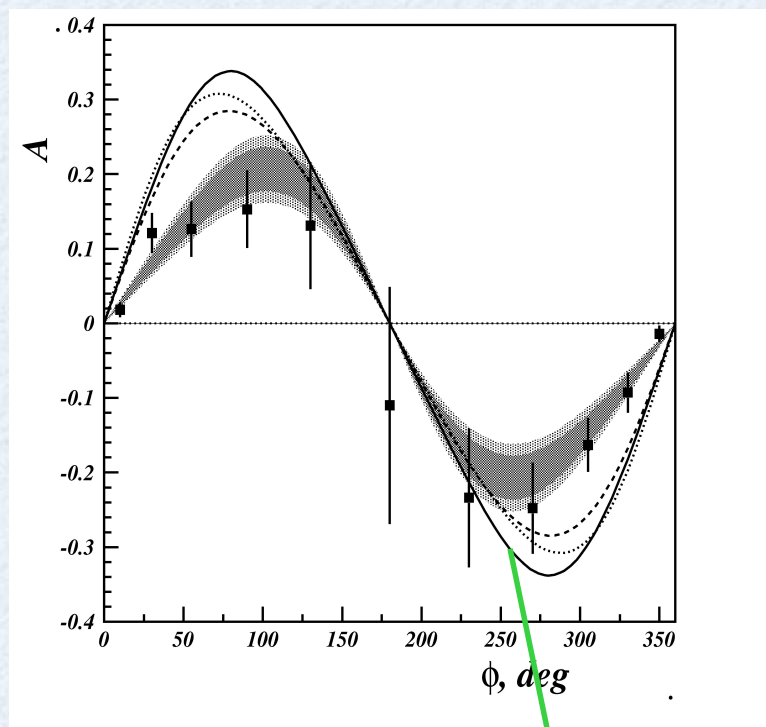
DVCS beam spin asymmetries: first observations around 2000

$$A_{LU} = \frac{(BH) * \text{Im}(DVCS) * \sin \Phi}{(BH^2 + DVCS^2)}$$

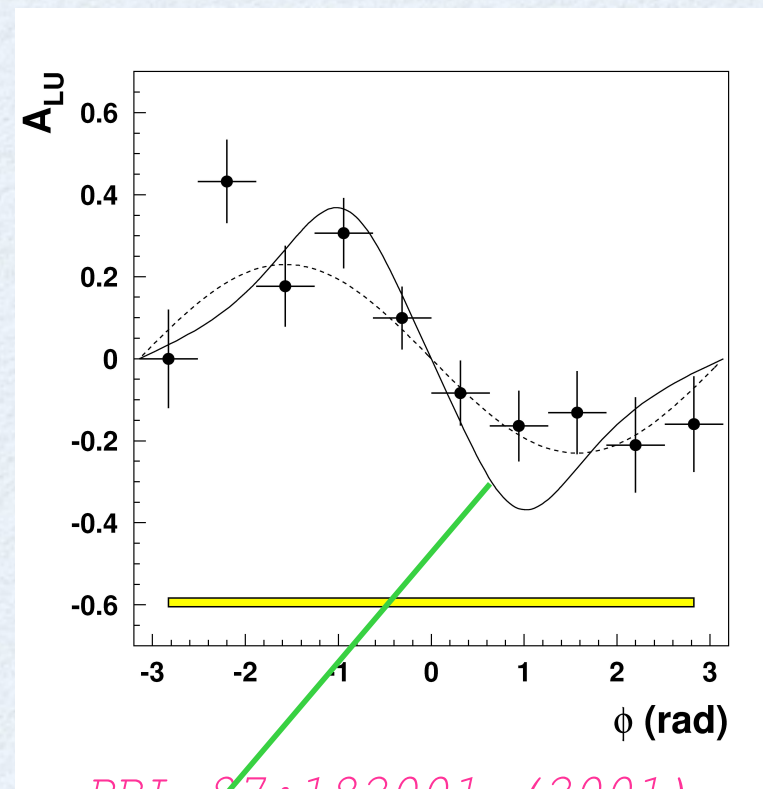


CLAS

$Q^2 = 1.25 \text{ GeV}^2$,
 $x_B = 0.19$,
 $-t = 0.19 \text{ GeV}^2$



PRL 87:182002 (2001)



PRL 87:182001 (2001)

HERMES

$Q^2 = 2.6 \text{ GeV}^2$,
 $x_B = 0.11$,
 $-t = 0.27 \text{ GeV}^2$

twist-2 + twist-3

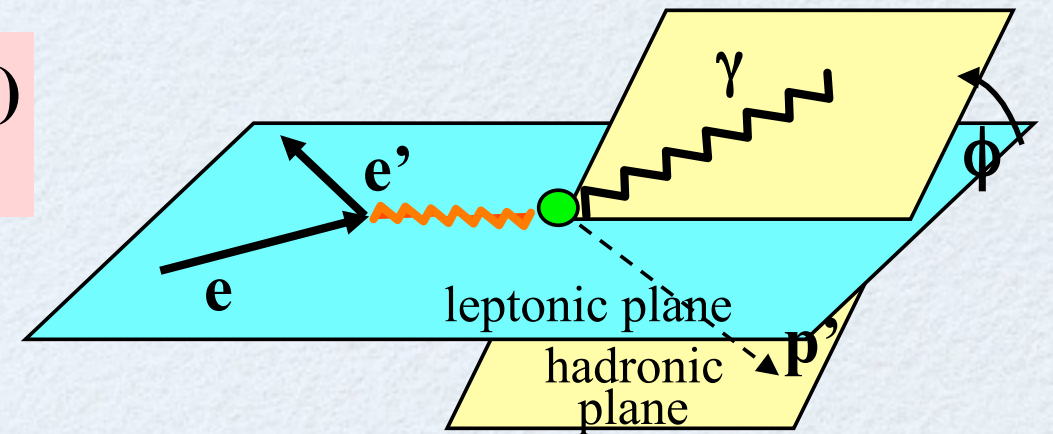
Vdh, Guichon, Guidal (1999)
Kivel, Polyakov, Vdh (2000)

DVCS observables

$$A = \frac{\sigma^+ - \sigma^-}{\sigma^+ + \sigma^-} = \frac{\Delta\sigma}{2\sigma}$$

$$\xi = xB/(2-xB)$$

$$k = -t/4M^2$$



Polarized **beam**, unpolarized **proton** target:

$$\Delta\sigma_{LU} \sim \sin\phi \operatorname{Im} \{ F_1 H + \xi(F_1 + F_2) \tilde{H} + kF_2 E \} d\phi$$

Kinematically suppressed

$$\rightarrow H_p, \tilde{H}_p, E_p$$

Unpolarized beam, **longitudinal proton** target:

$$\Delta\sigma_{UL} \sim \sin\phi \operatorname{Im} \{ F_1 \tilde{H} + \xi(F_1 + F_2)(H + \dots) \} d\phi$$

$$\rightarrow H_p, \tilde{H}_p$$

Unpolarized beam, **transverse proton** target:

$$\Delta\sigma_{UT} \sim \sin\phi \operatorname{Im} \{ k(F_2 H - F_1 E) + \dots \} d\phi$$

$$\rightarrow H_p, E_p$$

Polarized **beam**, unpolarized **neutron** target:

$$\Delta\sigma_{LU} \sim \sin\phi \operatorname{Im} \{ F_1 H + \xi(F_1 + F_2) \tilde{H} - kF_2 E \} d\phi$$

$$\rightarrow H_n, \tilde{H}_n, E_n$$

Suppressed because $F_1(t)$ is small

Suppressed because of **cancellation** between PPD's of u and d quarks

$$H_p(x, \xi, t) = 4/9 H_u(x, \xi, t) + 1/9 H_d(x, \xi, t)$$

$$H_n(x, \xi, t) = 1/9 H_u(x, \xi, t) + 4/9 H_d(x, \xi, t)$$

DVCS accesses Compton Form Factors: 8 CFFs at twist-2



$$\mathcal{H}_{Re}(\xi, t) \equiv \mathcal{P} \int_0^1 dx \left\{ \frac{1}{x - \xi} + \frac{1}{x + \xi} \right\} H_+(x, \xi, t)$$

$$\mathcal{H}_{Im}(\xi, t) \equiv H_+(\xi, \xi, t)$$

$$\tilde{\mathcal{H}}_{Re}(\xi, t) \equiv \mathcal{P} \int_0^1 dx \left\{ \frac{1}{x - \xi} - \frac{1}{x + \xi} \right\} \tilde{H}_+(x, \xi, t)$$

$$\tilde{\mathcal{H}}_{Im}(\xi, t) \equiv \tilde{H}_+(\xi, \xi, t)$$

and analogous
formulas for
GPDs E, \tilde{E}^q
respectively

with singlet GPD combinations
(quark + anti-quark):

$$H_+(x, \xi, t) \equiv H(x, \xi, t) - H(-x, \xi, t)$$

$$\tilde{H}_+(x, \xi, t) \equiv \tilde{H}(x, \xi, t) + \tilde{H}(-x, \xi, t)$$



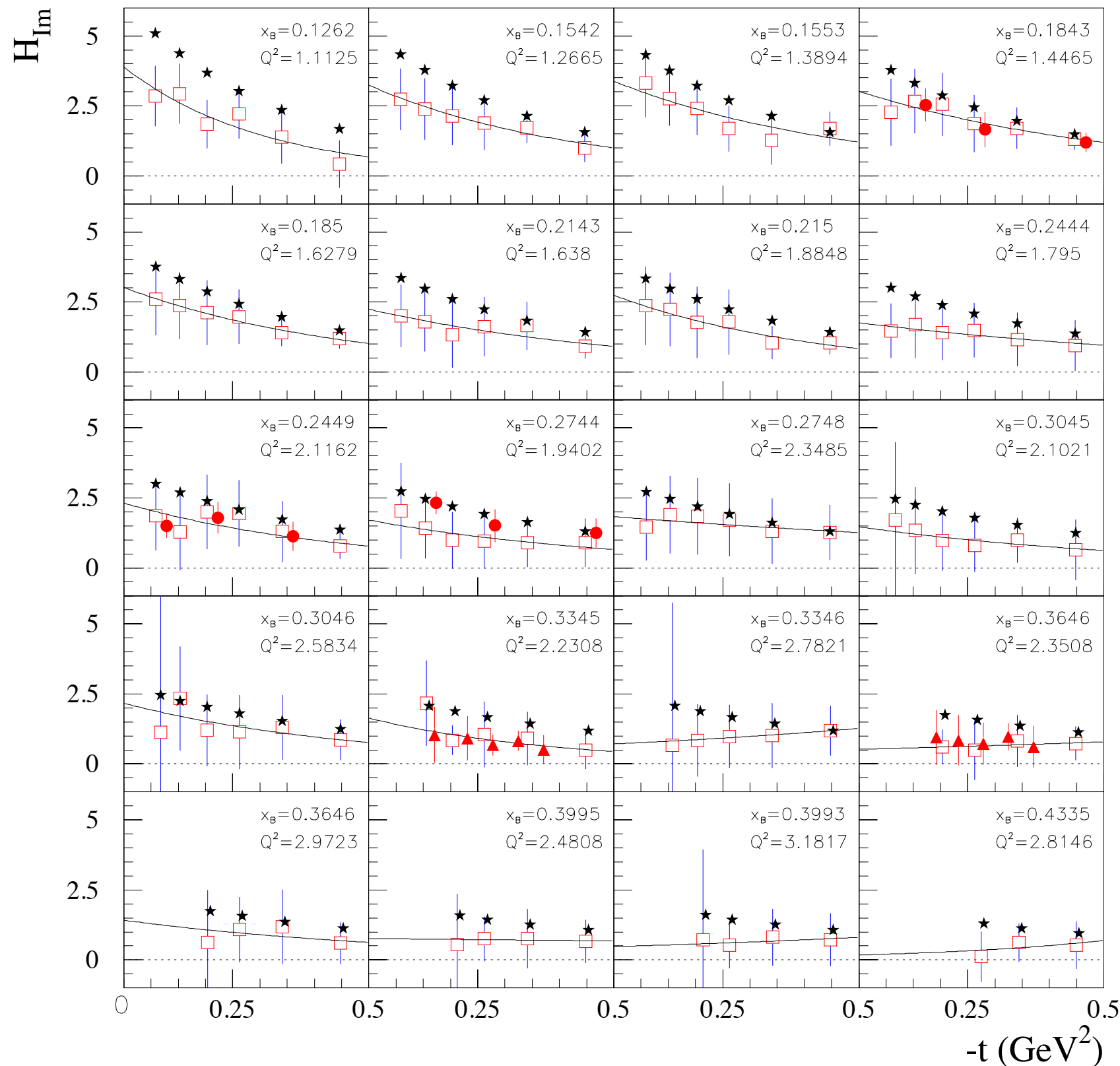
CFF fit extractions from data:

Guidal (2008, ...)

Guidal, Moutarde (2009, ...)

Kumericki, Mueller, Passek-Kumericki (2008, ...)

global analysis of JLab 6 GeV data



$$\mathcal{H}_{Im}(\xi, t)$$

red solid circles:
CLAS: σ , A_{LU} , A_{UL} , A_{LL}

red open squares:
CLAS: σ , A_{LU}

red triangles:
Hall A: σ , A_{LU}

black stars
VGG model values

Dupré, Guidal,
vdh (2017)

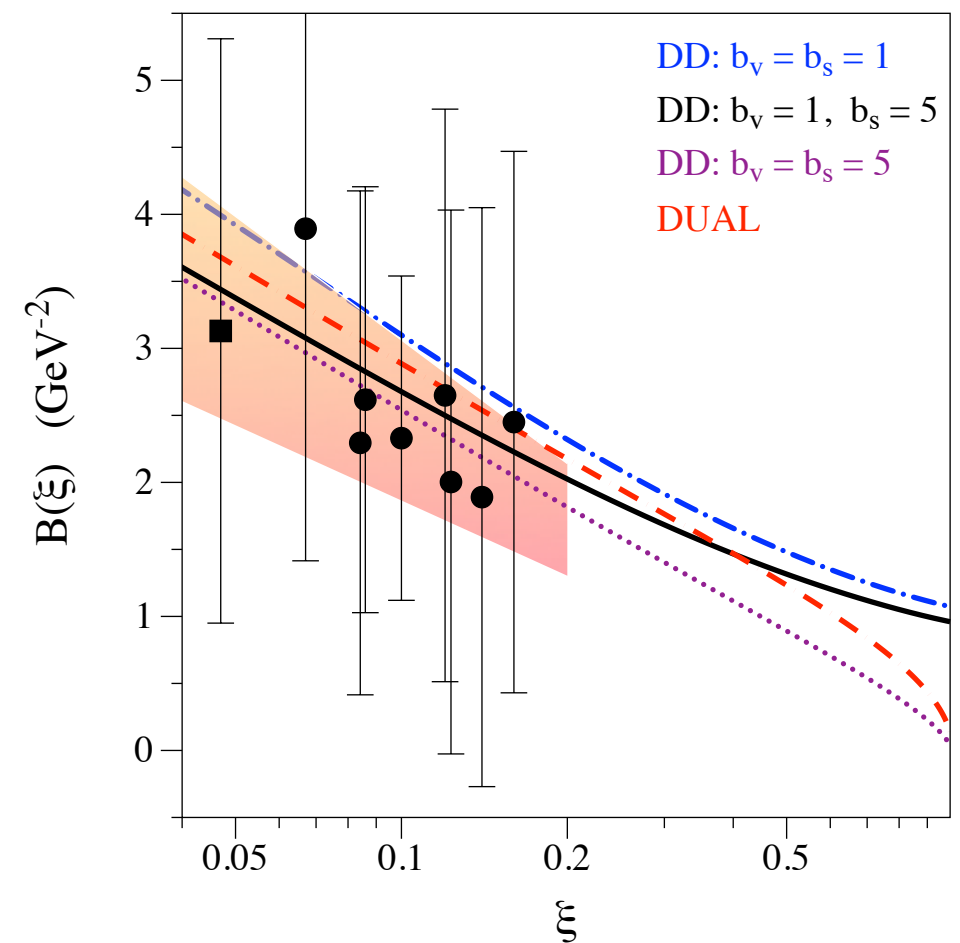
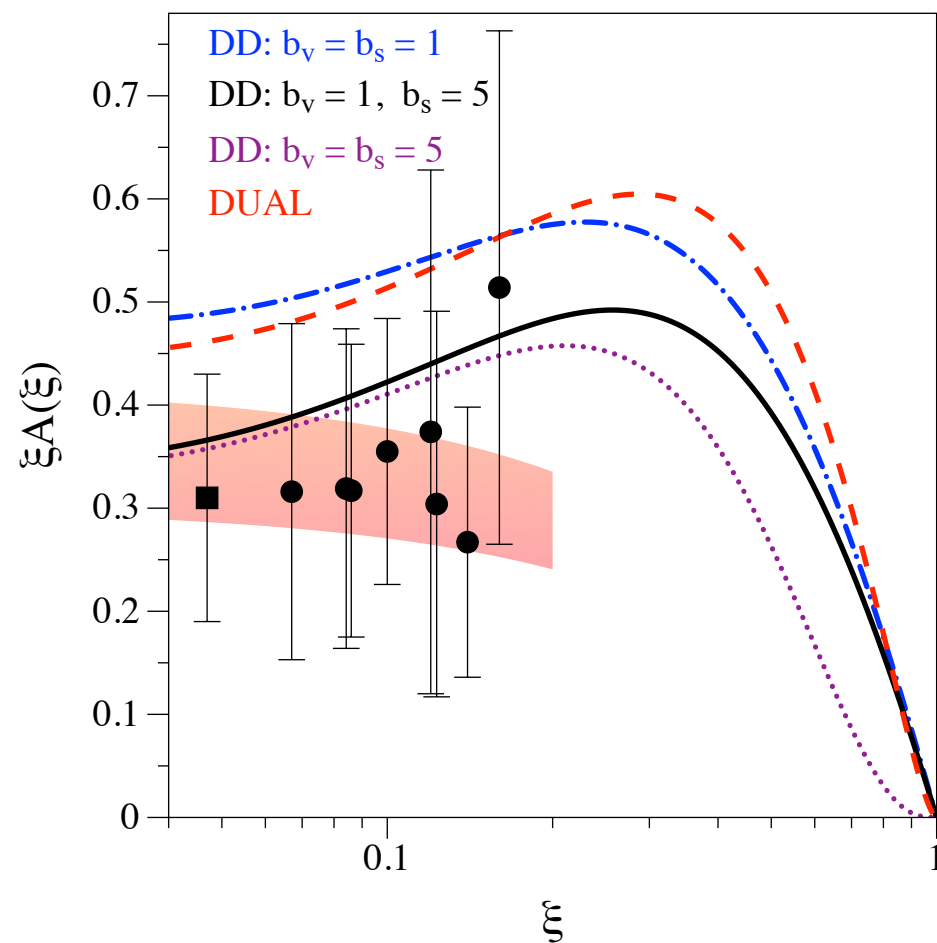
CFF \mathcal{H}_{Im} : $\mathcal{H}_{Im}(\xi, t) = A(\xi)e^{B(\xi)t}$

black circles: CFF fit of JLab data

Dupré, Guidal, Vdh (2017)

black squares: CFF fit of HERMES data

Guidal, Moutarde (2009)



$A(\xi) = a_A(1 - \xi)/\xi$

red bands:
1- parameter
fits of data

$B(\xi) = a_B \ln(1/\xi)$

3D imaging

$$\rho^q(x, \mathbf{b}_\perp) = \int \frac{d^2 \Delta_\perp}{(2\pi)^2} e^{-i\mathbf{b}_\perp \cdot \Delta_\perp} H_-^q(x, \xi = 0, -\Delta_\perp^2)$$

Burkardt (2000)

number density of quarks (q) with longitudinal momentum x
at a transverse distance \mathbf{b}_\perp in proton

non-singlet (valence quark) GPDs: $H_-^q(x, 0, t) \equiv H^q(x, 0, t) + H^q(-x, 0, t)$

x-dependent
radius

$$\langle b_\perp^2 \rangle^q(x) \equiv \frac{\int d^2 \mathbf{b}_\perp \mathbf{b}_\perp^2 \rho^q(x, \mathbf{b}_\perp)}{\int d^2 \mathbf{b}_\perp \rho^q(x, \mathbf{b}_\perp)} = -4 \frac{\partial}{\partial \Delta_\perp^2} \ln H_-^q(x, 0, -\Delta_\perp^2) \Big|_{\Delta_\perp=0}$$

$$H_-^q(x, 0, t) = q_v(x) e^{B_0(x)t} \longrightarrow \langle b_\perp^2 \rangle^q(x) = 4B_0(x)$$

x-independent
radius

$$\langle b_\perp^2 \rangle^q = \frac{1}{N_q} \int_0^1 dx q_v(x) \langle b_\perp^2 \rangle^q(x)$$

$N_u=2, N_d=1$

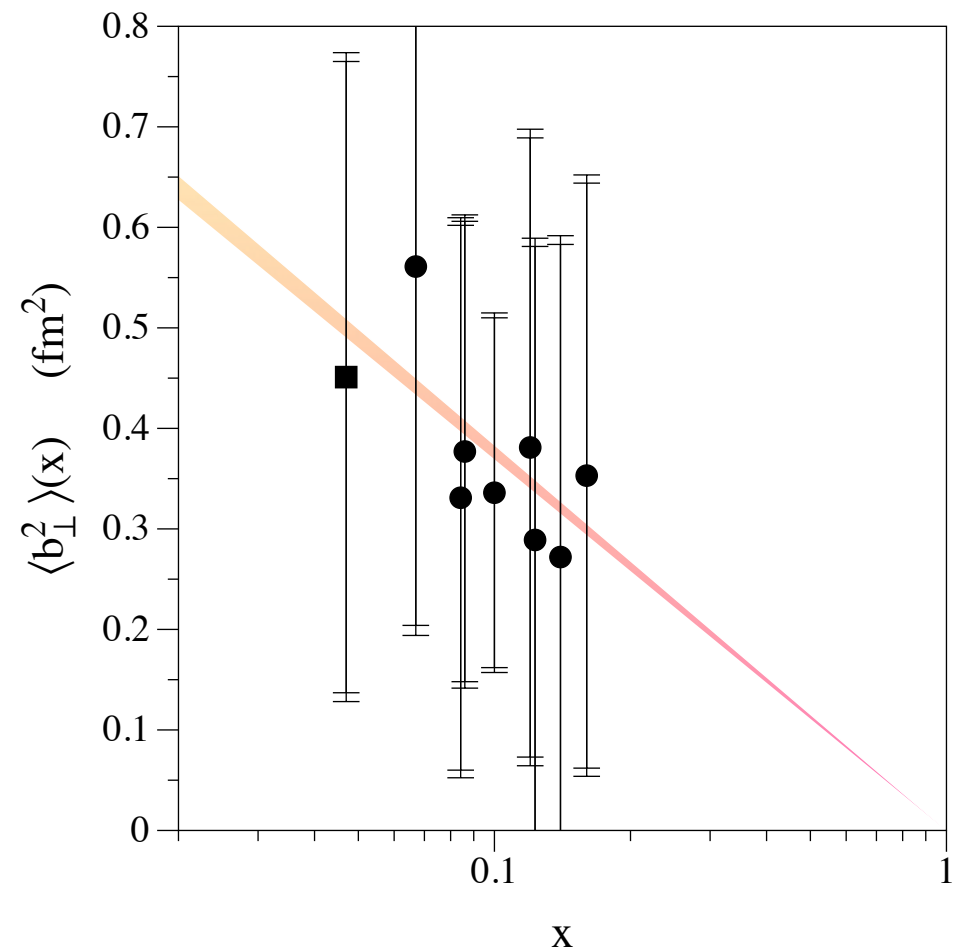
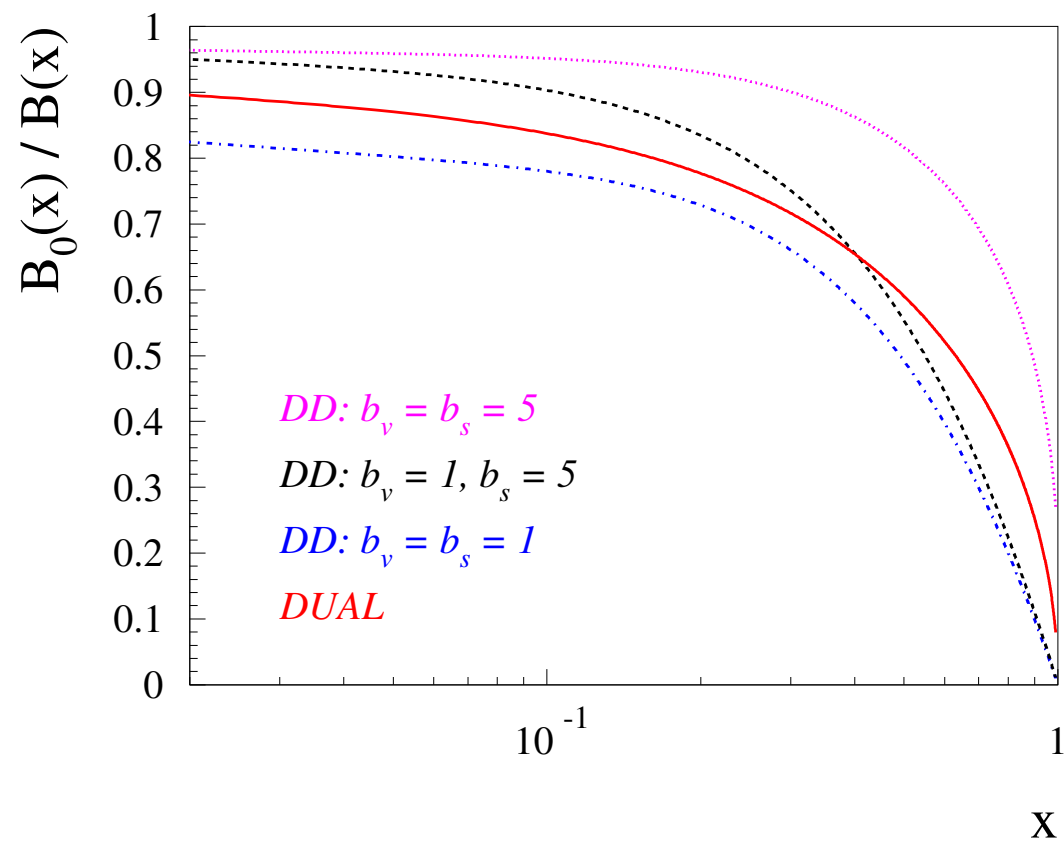
$$\langle b_\perp^2 \rangle = 2e_u \langle b_\perp^2 \rangle^u + e_d \langle b_\perp^2 \rangle^d = 2/3 \langle r_1^2 \rangle = 0.43 \pm 0.01 \text{ fm}^2$$

Bernauer (2014)

x-dependent radius in proton

black circles: CFF fit of JLab data

black squares: CFF fit of HERMES data



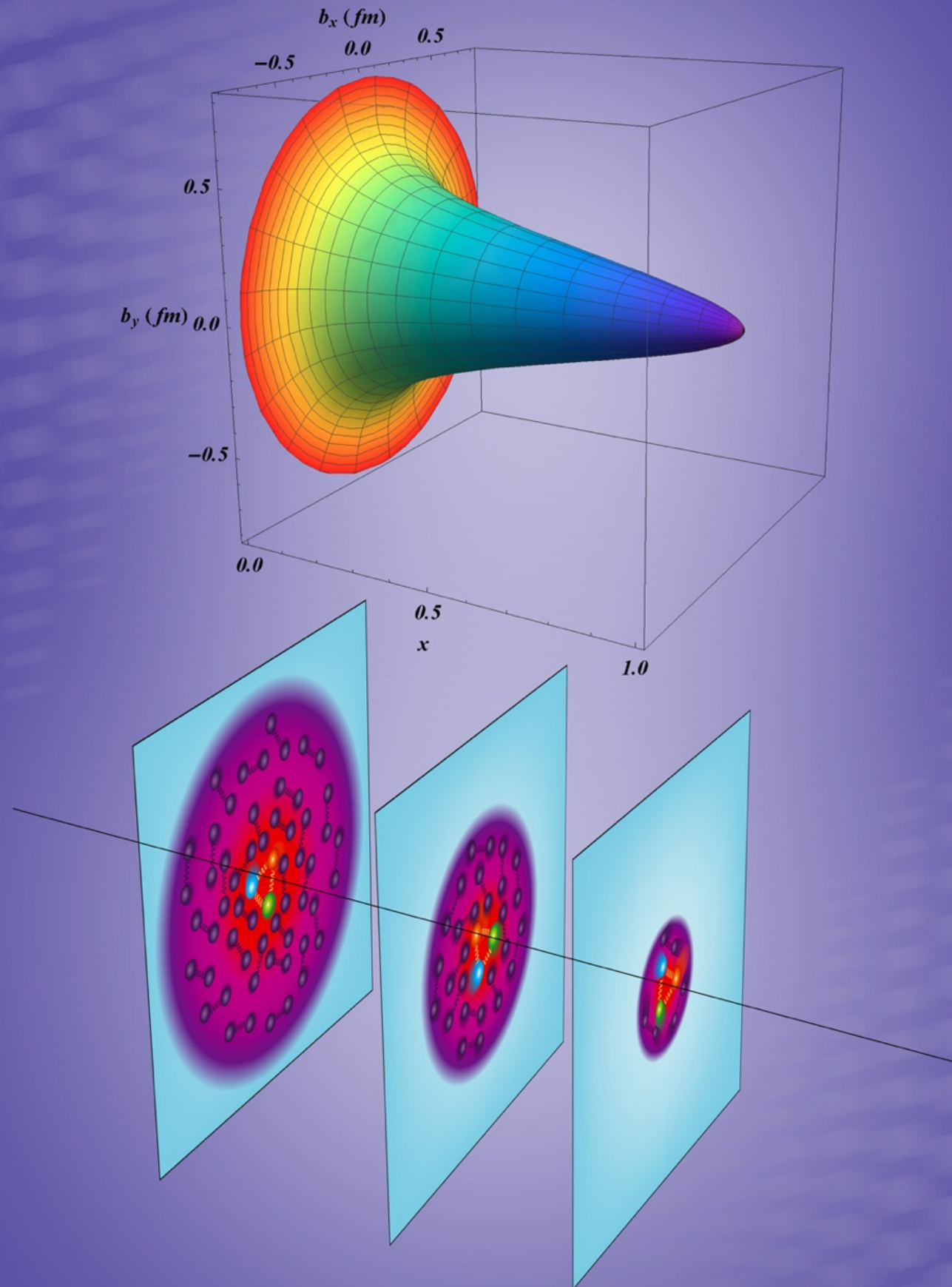
for $x < 0.15$: $B_0/B > 0.9$

band: using $B_0(x) = a_{B_0} \ln(1/x)$

a_{B_0} fixed from elastic scattering

Dupré, Guidal, Vdh (2017)

3D imaging of proton



Dupré, Guidal, Vdh (2017)

CFF \mathcal{H}_{Re} : dispersion relation formalism

Anikin, Teryaev (2007)

Diehl, Ivanov (2007)

Polyakov, Vdh (2008)

Kumericki-Passek, Mueller, Passek (2008)

Goldstein, Liuti (2009)

Guidal, Moutarde, Vdh (2013)

➔ once-subtracted fixed-t dispersion relation

$$\mathcal{H}_{Re}(\xi, t) = -\Delta(t) + \mathcal{P} \int_0^1 dx H_+(x, x, t) \left[\frac{1}{x - \xi} + \frac{1}{x + \xi} \right]$$

ξ -independent
subtraction function

known from CFF
 $\mathcal{H}_{Im}(x, t)$

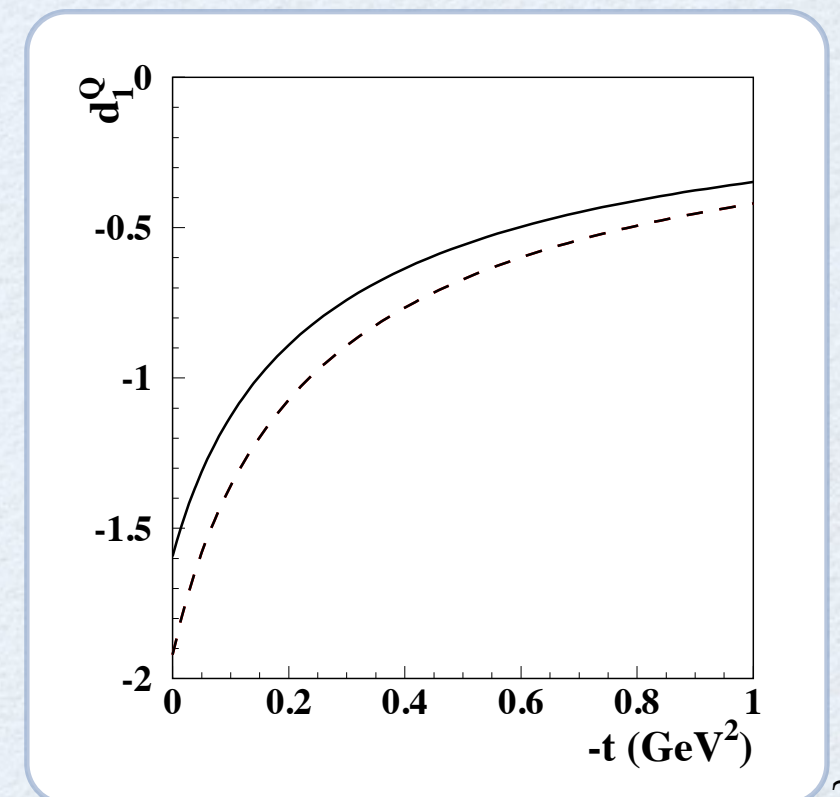
Pasquini, Polyakov, Vdh (2014)

$$\Delta(t) \equiv \frac{2}{N_f} \int_{-1}^1 dz \frac{D(z, t)}{1 - z}$$

D-term

$$D(z, t) = (1 - z^2) \sum_{\substack{n=1 \\ n \text{ odd}}}^{\infty} d_n(t) C_n^{3/2}(z)$$

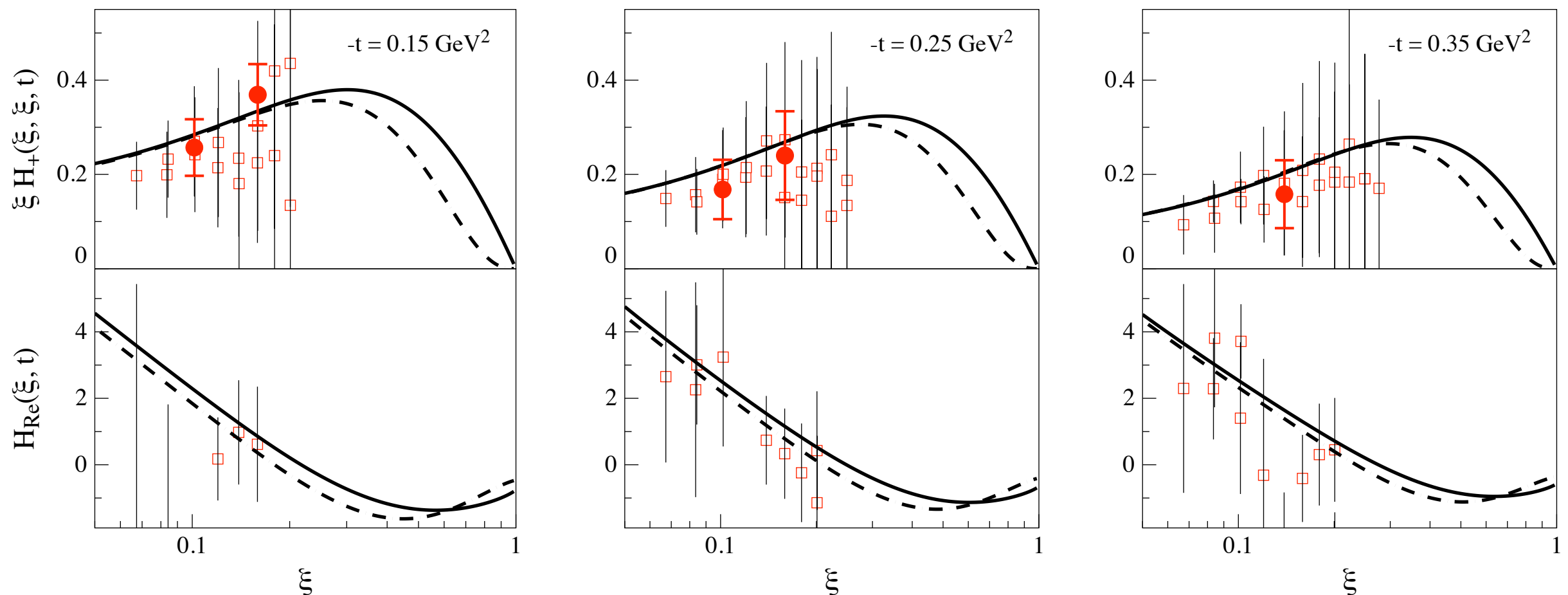
Polyakov, Weiss
(1999)



experimental strategy for CFF \mathcal{H}_{Re} : direct extraction vs dispersion formalism

red solid circles: CLAS: σ , A_{LU} , A_{UL} , A_{LL}

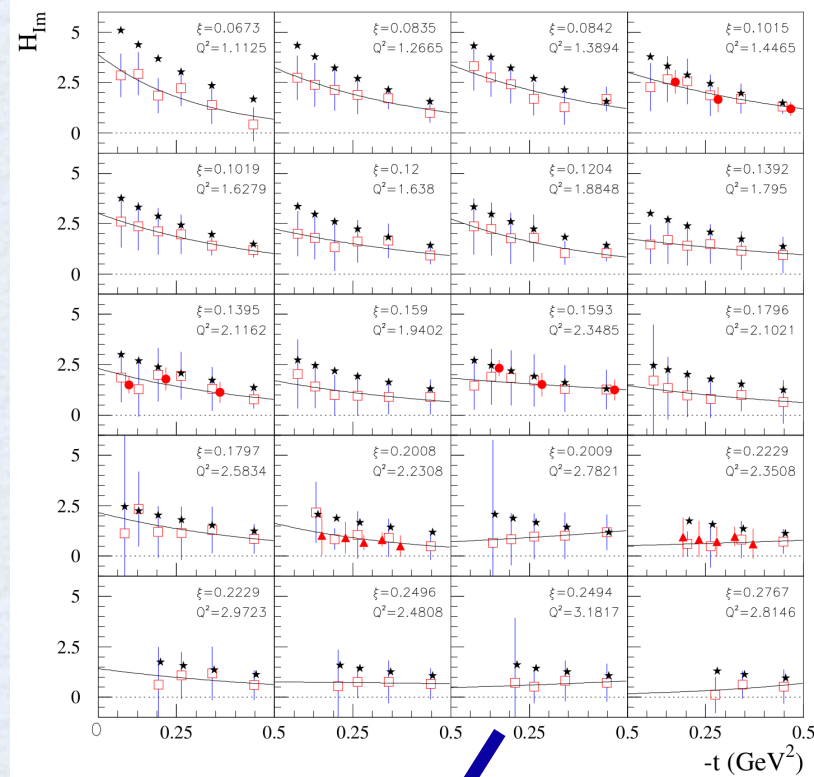
red open squares: CLAS: σ , A_{LU}



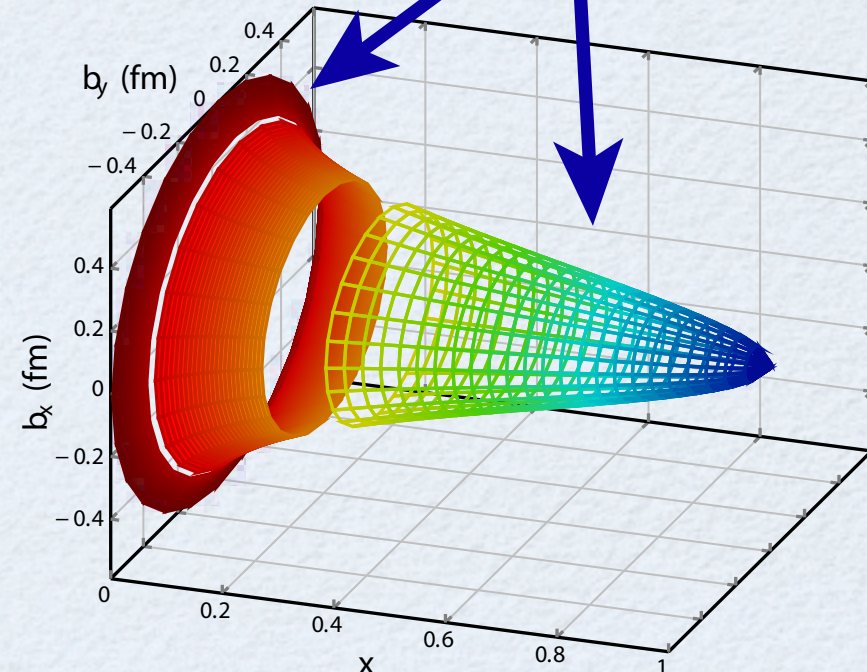
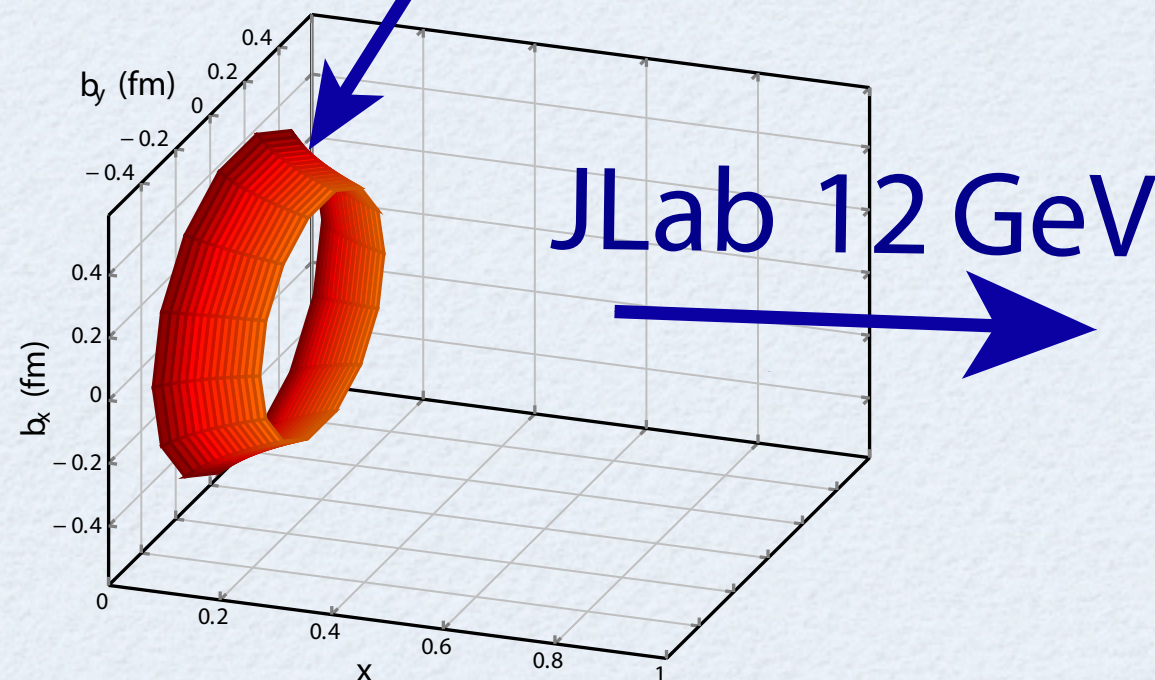
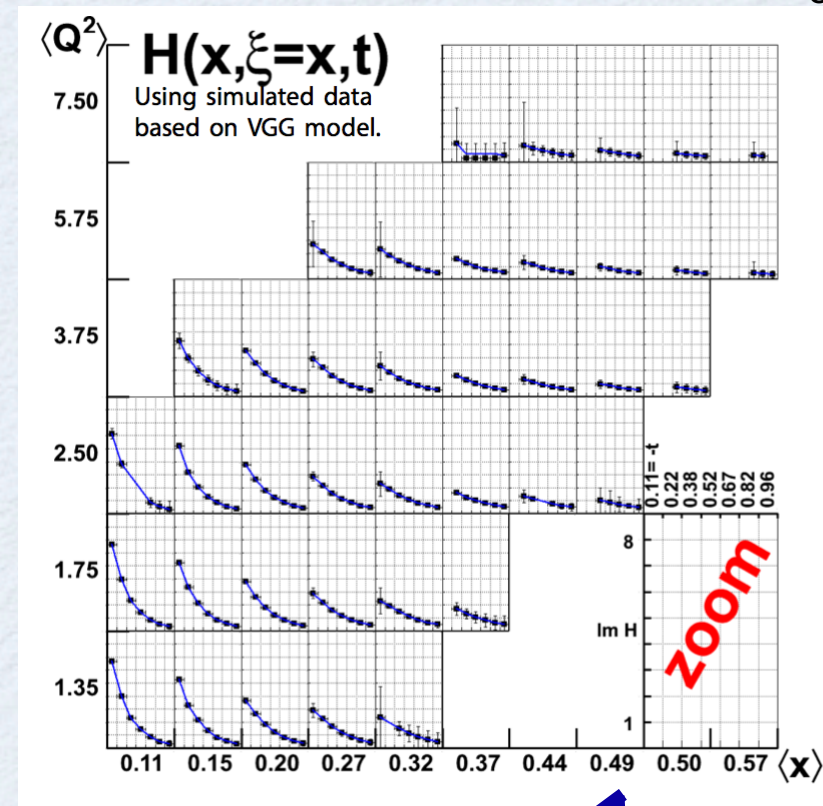
Dupré, Guidal, Niccolai, Vdh (in progress)

Projections for CFFs at JLab 12 GeV

Düpré-Guidal-Vanderhaeghen-PRD **95** 011501 (R) (2017)



CLAS12 projections E12-06-119 with DVCS A_{UL} and A_{LU}



JLab 12 GeV

courtesy of Z.E. Meziani

Outlook

- ➔ elastic / transition FFs have allowed to get a first glimpse at the spatial distributions of quarks in nucleons
- ➔ GPDs allow for a proton imaging in longitudinal momentum and transverse position
- ➔ global analysis of JLab 6 GeV data have shown a proof of principle of such 3D imaging (tools available: fitters, dispersive analyses)
- ➔ systematic 3D imaging is possible now: COMPASS, JLab 12 GeV,...EIC

